AN ABSTRACT OF THE THESIS OF

__Yang Sun__ for the degree of _____Master of Ocean Engineering_____

in _____Civil Engineering_____ presented on _____June 30, 1992_____

Title: ____Nonlinear Dynamic Response of Cable/Lumped-Body System by Direct____

_____Integration with Suppression_____

Abstract approved:__ ## Redacted for Privacy

Dr. John W. Leonard

An improved algorithm for simulation of the three-dimensional nonlinear hydrodynamic behavior of a cable/lumped-body system is developed based on a direct integration method with suppression of extraneous erroneous solution.

The governing equations of the cable continuum with dependent variables of cable velocities, direction cosines and tension magnitude are derived from the dynamic equilibrium conditions and kinematic compatibility conditions. The equations of motion of boundary and intermediate bodies are treated as boundary conditions and internal boundary conditions ,respectively.

The nonlinear combined initial-value and boundary-value problem is then solved in the time-domain by introducing a stable Newmark-like implicit integration scheme in time. This transforms the problem into a nonlinear quasi-static two-point boundary-value problem.

The spatial integration algorithm is a semi-analytical method. The boundary-value problem, posed as a set of nonlinear partial differential equations, is first transformed into an iterative set of quasi-linearized boundary-value problem. The quasi-linearized boundary value problem is then further decomposed into a set of quasi-linearized initial-

value problems in the spatial coordinate so that numerical integration can be performed along the cable from one end to the other. A suppression algorithm is developed to effectively control the growth of extraneous erroneous solutions during the numerical integration of the partial solutions to each of the initial-value problems. The partial solutions are recombined at the terminal end in order to satisfy the boundary conditions.

A set of sample problems are presented to demonstrate the validity and capability of the theoretical formulation and solution algorithms. The present study provides a favorable comparison between numerical predictions and analytical or experimental results. The suppression technique is shown to be an efficient and useful tool in improving the direct integration method of simulation of cable/lumped body systems.

Nonlinear Dynamic Response of Cable/Lumped-Body System
by Direct Integration with Suppression

by

Yang Sun

A THESIS

Submitted to

Oregon State University

in partial fulfillment of
the requirements for the
degree of

Master of Ocean Engineering

Completed June 30, 1992
Commencement June 1993

APPROVED:

Professor of Civil Engineering in charge of major

Head of Department of Civil Engineering

Dean of Graduate School

Date thesis is presented _____ June 30, 1992 _____

Typed by Ping Zhang for _____ Yang Sun _____

ACKNOWLEDGEMENTS

<div style="text-align: right">Yang Sun</div>

TABLE OF CONTENTS

TABLE OF CONTENTS (continued)

TABLE OF CONTENTS (continued)

LIST OF FIGURES

LIST OF TABLES

NONLINEAR DYNAMIC RESPONSE OF CABLE/LUMPED-BODY SYSTEM

BY DIRECT INTEGRATION WITH SUPPRESSION

1.0 INTRODUCTION

1.1 Background

The Naval Civil Engineering Laboratory (NCEL) as part of its efforts in the Advanced Ocean Ranges (AOR) project has identified several technical problems in the efficient design and installation of cable/lumped body systems at predetermined bottom positions in deep sea waters. Two of those problems are 1) the necessity to predict optimum installation parameters with given constraints and performance; 2) the necessity to predict corrective procedures during installation. The key to achieve these objectives lies in the development of a three dimensional deterministic analysis program for predicting the dynamic behavior of cable/lumped-body system subject to ocean environmental loadings (Leonard,1989).

A cable/lumped body system is comprised of a buoy or boundary body, mooring lines connecting the buoy and intermediate bodies located at intermediate points along the cable scope and either an anchor to the sea-bottom or a winch on the ship. The mooring lines consist of cable segments that may have different geometry and material properties. The cable segments are three dimensional curved, slender, flexible cylinders with no bending stiffness. Buoys or bodies may have various geometries depending on their different functions. Factors that should be considered in the modelling of the buoys or bodies include: wave induced force models for small

and large buoys and coupling of loading and response; three dimensional character of system response; the nonlinear rotational degrees of freedom; the buoy-sea-air interface. The loadings acting on the system are, in addition to dead load due to gravity, environmental loadings from buoyancy, winds, hydrodynamic loads, and a variety of live loads peculiar to its application. Hydrodynamic loadings devolve from both surface waves and non-uniform currents from arbitrary directions. The live load may result from time varying concentrated loads or excitations imposed on the bodies. The boundary conditions can be divided into two types: 1) kinematic boundary conditions at the boundary points where velocities are specified by the known conditions of the problem such as anchoring, maneuver of installation vessel, and cable payout; and 2) force boundary conditions from dynamic equilibrium equations at the boundary or intermediate bodies.

The analysis of such ocean cable systems is difficult. Firstly, the stiffness of the cable system depends on the displacement of the system. When in a slack configuration, the stiffness of the system may nearly vanish and its behavior becomes highly nonlinear. Secondly, nonlinearities are introduced by hydrodynamic drag force terms on the cable and bodies which vary with the cable orientation as well as quadratically in magnitude of the relative flow. Hydrodynamic forces are also position dependent and even linear waves will introduce nonlinear geometric changes in the system configuration (Leonard and Tuah,1986). Further, the position and orientation changes in the cable segments adjoining the body will cause nonlinear interactions of the mooring line and the bodies. Other nonlinearities may be attributed to material

simulate the three dimensional maneuver of vessels, shear and rotary currents and crossing seas, and three dimensional character of buoy response, all of which effect the performance of the system. A three dimensional analysis complicates the problem by an order of magnitude and could result in a computer program that may not run efficiently on a IBM-PC/AT or compatible.

1.2 Review of Previous Studies

Research has been ongoing since 1987 at Oregon State University under the auspices of NCEL and ONR to develop a dynamic response simulation method for the cable/lumped body system. A FORTRAN program named KBLDYN was developed by Chiou in 1989 for modelling the three-dimensional nonlinear dynamic behavior of such systems. His work was summarized in his Ph.D. dissertation entitled "Nonlinear Hydrodynamic Response of Curved Singly-Connected Cables" (Chiou,1989).

In his work, the governing equations of motion of a cable continuum are derived from the dynamic equilibrium equations and the kinematic compatibility equations. The equations of motion of boundary bodies serve as the boundary conditions of the segmented boundary-value problem. The equations of motion of intermediate bodies are considered as the internal boundary conditions of the boundary-value problem. The governing equations of cable and the boundary conditions constitute a nonlinear combined initial-value and boundary-value problem.

The time-domain approach based on an implicit integration scheme was adopted in KBLDYN to deal with time varying loads on the cable/buoy system

(Leonard,1988; Wang,1977; Chiou,1989). The time domain approaches, unlike the frequency-domain approaches (Clough and Penzien,1975; Leonard,1988), do not require linearity of the response. Although time-domain approaches are not as computational efficient as frequency-domain approaches, they provide better estimates of nonlinear responses. Also, nonlinear responses can be modelled by direct integration in time of the equations of motion of selected points in the system.

Different direct integration algorithms can be adopted, explicit or implicit, to propagate solutions from one time step to the next (Bathe,1984). The explicit methods do not require iterative solutions of equations to determine solutions at a given time and are more computational efficient for a single time step. However, the solutions are conditionally stable depending on the time step size and, thus, overall computational efficiency is lost for long reaches of integration. The further problem of numerical drift of solutions has been pointed out by Wang (1984). Chiou (1989) used an implicit method based on a backward finite difference formula. It is unconditionally stable and enables use of very large time steps (consistent with the variability of the loads) and is better suited for longer reaches of integration. Iterative procedures are required at each time step which implies more computational time for each real time step. Once the implicit method is used, the problem is transformed into an equivalent "static" two-point nonlinear boundary-value problem along the cable at every time instant.

Numerical spatial discretization of the cable is required for realistic loading conditions. Three classes of discretization are prevalent (Leonard and Nath,1988):

Lumped Parameter Method (LPM); Finite Element Method (FEM) and Direct Integration Method (DIM).

The LPM and FEM represent the cable as a series of discrete elements with nodes and degrees of freedom at the end of each element (Delmer,1988; Thresher and Nath,1975; Leonard and Nath,1981; Liu,1977,1982). The greater the number of degrees of freedom, the greater the accuracy of response and the greater the computational time required. For two-dimensional problems, the computer memory provided by a microcomputer will suffice. For three-dimensional problems, the number of degrees of freedom required in the LPM and FEM models may be a limitation in using microcomputers. The LPM assumes that all loads, parametric effects and responses are lumped at the nodes (Leonard and Nath 1981, Wang 1977) and usually an explicit integration method is used to integrate the equations in the time domain. This leads to an efficient solution if the time step required for stability is not too small.

The FEM does not make as many assumptions as the LPM regarding the properties and behavior of the cable and considers effects integrated over the lengths of the elements (Leonard and Nath 1981, Webster 1975). In fact the LPM can be considered a simplified subset of the FEM (Wang 1977). In the FEM, coupled equations for the degrees of freedom are obtained. There are several general purpose structural analysis programs based on the finite element method which have been considered for buoy system analysis (Webster 1975, Leonard and Tuah 1986). The use of such programs for singly-connected mooring legs requires a significant

computational time in that numerous degrees of freedom at nodal points along the cable must be introduced and calculated over the time history of response. Difficulties have been reported for FEM programs used for buoy system analysis when disparate stiffness between cable elements and buoys are present (Webster and Palo 1986). Also difficulties are anticipated when nearly inextensible cables are present.

In the DIM, coupled first-order differential equations for the spatial distribution of behavior are numerically integrated along the scope of the cable (Leonard 1979, Chiou 1985, 1989). Variable parameters and loads along the scope can then be easily handled and extremely accurate predictions of response are possible. Since intermediate nodes and degrees of freedom along the scope are not required as in the LPM and FEM, considerable savings in computational expense are possible because solutions of large sets of simultaneous equations are not required. Further, considerably less computer memory storage is required and, hence, the code can be used aboard the installation vessel where large computer system may not available.

In KBLDYN, the spatial direct integration is a semi-analytical method. The boundary-value problem, posed as a set of nonlinear partial differential equations, are first transformed into an iterative set of quasi-linear boundary-value problems. The quasi-linear boundary-value problem is then further decomposed into a set of linear initial-value problems so that numerical integration may be performed along the cable from one end to the other. The solutions to each of the initial-value problem, hereafter called "partial solutions", are recombined so as to satisfy the boundary conditions. The nonlinear boundary-value problem is then solved by successive iterations.

(Chiou,1989)

The numerical method developed in Chiou's work has been demonstrated and validated by comparison to solution accuracies and computation times for representative cable problems treated with other solution methods and by comparison to experimental results and therefore has been selected as the base model for the dynamic response simulation program of AOR project (Harris and Shields,1990).

However,as reported by Chiou (1989), some difficulties were encountered during the test of the program KBLDYN:

1) Divergence or overflow occurred for some particular problems. The solutions to the governing equations of the cable system are of exponential type. When using the direct integration method, the numerical solutions may grow very fast as the integration is carried out along the cable length. If the closed form solutions were available, the coefficients of the exponential solutions with positive exponents would be equated to zero by satisfying the boundary conditions at the terminal end . However, for the direct integration scheme adopted in KBLDYN the erroneous growth of the numerical solutions may become out of control during the numerical integration of the partial solutions of the quasi-linear initial-value problem. That is to say, the exponential terms in the partial solutions grow rapidly along the cable length before reaching the terminal end where the erroneous partial solutions are to be suppressed by applying boundary conditions. This may result in ill-conditioned boundary conditions at the terminal end and cause larger and larger errors during the Newton-Raphson iteration process. It was found that such erroneous growth rates of partial

solutions are proportional to the spatial integration step size ΔS, to the inverse of the tension T, to the inverse of time step size Δt and to the velocity change within each time step ΔV. Therefore, difficulties arise when: a) the problem contains long cable lengths; b) low tension regions appear within the cable scope; c) a small time step is required to predict the response of a system with high-frequency excitation; and d) near the buoy or tow point where the velocity of the cable may have dramatic change or near cable material discontinuity points where rapid changes in cable curvature may occur.

2) Numerical damping and numerical drift were noticed. The numerical integration scheme based on the backward difference formula uses only the information of known velocities at the previous time step to predict the unknown acceleration at the present time. Although it is an unconditionally stable method, it provides an estimate of the acceleration with less accuracy based solely on the previous time and thus introduces numerical damping into the solution. The existence of numerical damping may lead to an inaccurate prediction of long term response and prevent it from being incorporated into a dynamic optimization and control program for the cable/body installation based on the "time decrement method", i.e. given a final desired state for all variables, use small steps backward in time to predict the solutions at previous times to achieve that final desired state (Leonard,1989).

3) The potential singularity, i.e. T=0, exist throughout the governing equations. Thus, difficulties may arise when dealing with some special boundary conditions during the cable/lumped body installation procedures such as cable free end

boundary conditions and slack-cable/ocean-bottom contact boundary conditions in which singularities exist either at the cable tip or at the touchdown point.

It is the intent of this work to develop an improved theoretical formulation and numerical algorithms to overcome the difficulties described above. The primary research interest focuses on developing a numerical method to alleviate the difficulties encountered in the direct integration of the partial solutions to each quasi-linearized initial-value problem.

There are two methods considered to be applicable to achieve this purpose. One method, the multi-segment method, was first developed in analyzing static and dynamic behavior of nonuniform conical shells (Goldberg and Bogdanoff,1961) and was later applied to the direct numerical integration for the large defection analysis of elastic-plastic shells of revolution (Gerdeen,1970). The method consists of subdividing the integration region into short segments. The initial-value problems are integrated within each segment, and solutions are combined to satisfy compatibility requirements at the junctions of the various segments. The second method, the suppression method (Goldberg, 1961; Zarghamee and Robinson, 1965), was used by Carter, Robinson and Schnobrich (1969) and by Leonard (1969) for the dynamic response of elastic shells. The method consists of combining the partial solutions at computer-selected points along the region in order to suppress the extraneous solutions. The suppression method is implemented by requiring that at certain spatial points fictitious conditions be satisfied by linear combinations of the unsuppressed partial solutions. The fictitious conditions to be satisfied must be arbitrary,

independent conditions which have small magnitudes compared with the partial solutions. The partial solutions are therefore combined to form new arbitrary partial solutions in which the extraneous growing functions are suppressed. The linear combinations at the point of suppression and at all prior points constitute the new set of arbitrary solutions which are then propagated along the integration path to the next point at which suppression is required. Although the two methods are similar in concept, and although the multi-segment method lends itself to an easier physical interpretation, the suppression method seems to have more advantages over the multi-segment method. First of all, in the multi-segment method the selection of the size of each segment is the only way to control the growth of the extraneous erroneous solution. In the suppression technique the growth of the extraneous solutions is controlled based on a criteria imposed on the growth of the selected dependent variables. The choice of the suppression points is then arbitrary and the suppression points can be unevenly spaced. Also, the suppression method requires much less computation than that of multi-segment method. Instead of solving, for example, one set of 3N equations simultaneously, N sets of 3 simultaneous equations are solved successively. For the above reasons the suppression method was chosen in this study.

1.3 Objectives of Present Study

The objectives of this study can be summarized as follows:

1) Set up a new formulation with dependent variables of cable velocities, direction cosines and tension magnitude such that the potential

singularities,i.e. T=0, are localized in the governing equations for the direction cosines. This may provide benefit when dealing with some particular boundary conditions where a singularity exists.

2) Investigate the numerical difficulties encountered by KBLDYN and develop a suppression scheme to effectively control the growth of extraneous erroneous partial solutions during the direct numerical integration along the cable length in order to provide an improved solution algorithm of direct integration method.

3) The implicit integration scheme based on the backward difference formula for time integration will be modified to eliminate the numerical damping that is present in KBLDYN. A new implicit integration scheme based on a Newmark-like method will be adopted.

4) Investigate the treatment of special boundary conditions such as payout boundary conditions,free end boundary conditions and cable/ocean-bottom contact boundary conditions that may encountered during the cable/body installation procedures.

5) Validate, by a set of sample example,the new formulation and numerical algorithms by comparing the numerical results to available analytical solutions or experimental data.

1.4 Scope of Study

In this study an improved theoretical formulation and solution algorithms based on direct integration method for the three-dimensional nonlinear dynamic analysis of

cable/lumped body system subject to hydrodynamic loads are presented.

In Chapter 2, the basic assumptions made to mathematically model the cable-body system are summarized. The governing equations of motion of the cable/lumped body system, with dependent variables of cable velocities, direction cosines and tension magnitude, are then derived so as to form a nonlinear combined initial-value and boundary-value problem. A set of Newmark-like formulas are presented to provide a implicit time integration scheme without numerical damping. Once the implicit integration scheme is adopted, the problem is transformed into an equivalent "static" nonlinear two-point boundary-value problem at every time instant.

The numerical methods,including the Newton-Raphson quasi-linearization, the decomposition of quasi-linear two-point boundary-value problem and the suppression technique are reviewed in Chapter 3. The solution algorithm and implementation procedures are then developed by applying these numerical methods to the cable/body system. The emphasis is placed on developing a suppression technique and incorporating it into the solution algorithm for the cable/body system to provide an improved, more stable direct integration method. The general solution algorithm is presented at the end of Chapter 3.

A set of sample problems are given in Chapter 4 to validate and demonstrate the present theoretical formulation and solution algorithms. Chapter 5 contains conclusions and recommendations resulting from this study.

2.0 GOVERNING EQUATIONS AND BOUNDARY CONDITIONS

The general definition sketch of the cable system in this study is shown in Fig.2.1. The X_i (i=1,2,3) frame is a global coordinate system, and S is the local coordinate along the cable scope. Let ξ be an arbitrary material point on the cable at some distance S from one end of the cable, and dS be an infinitesimal arc length along the cable. The position coordinates, $X_i(s,t)$, velocity components $\dot{X}_i(s,t)$ and tension components $T_i(s,t)$ (or direction cosines $\phi_i(s,t)$) are desired under the hydrodynamic loadings from surface waves and the subsurface currents in time domain,t. Through out the study, the term "boundary body" is used when referring to the discrete package at either end of the singly-connected cable system. The word "joint" refers to the point where two adjacent cable segments meet. The term "intermediate body" refers to a package at a joint.

In Section 2.1., the basic assumptions of the present model are summarized. The basic relationships are provided in Section 2.2. Section 2.3 contains the description of the external loads on the cable/body system. The governing equations of the system are derived in Section 2.4. The various boundary conditions are specified in Section 2.5. In Section 2.6, the implicit integration scheme is introduced. Thus, a two-point boundary-value problem posed by a set of quasi-static governing equations and boundary conditions is formed.
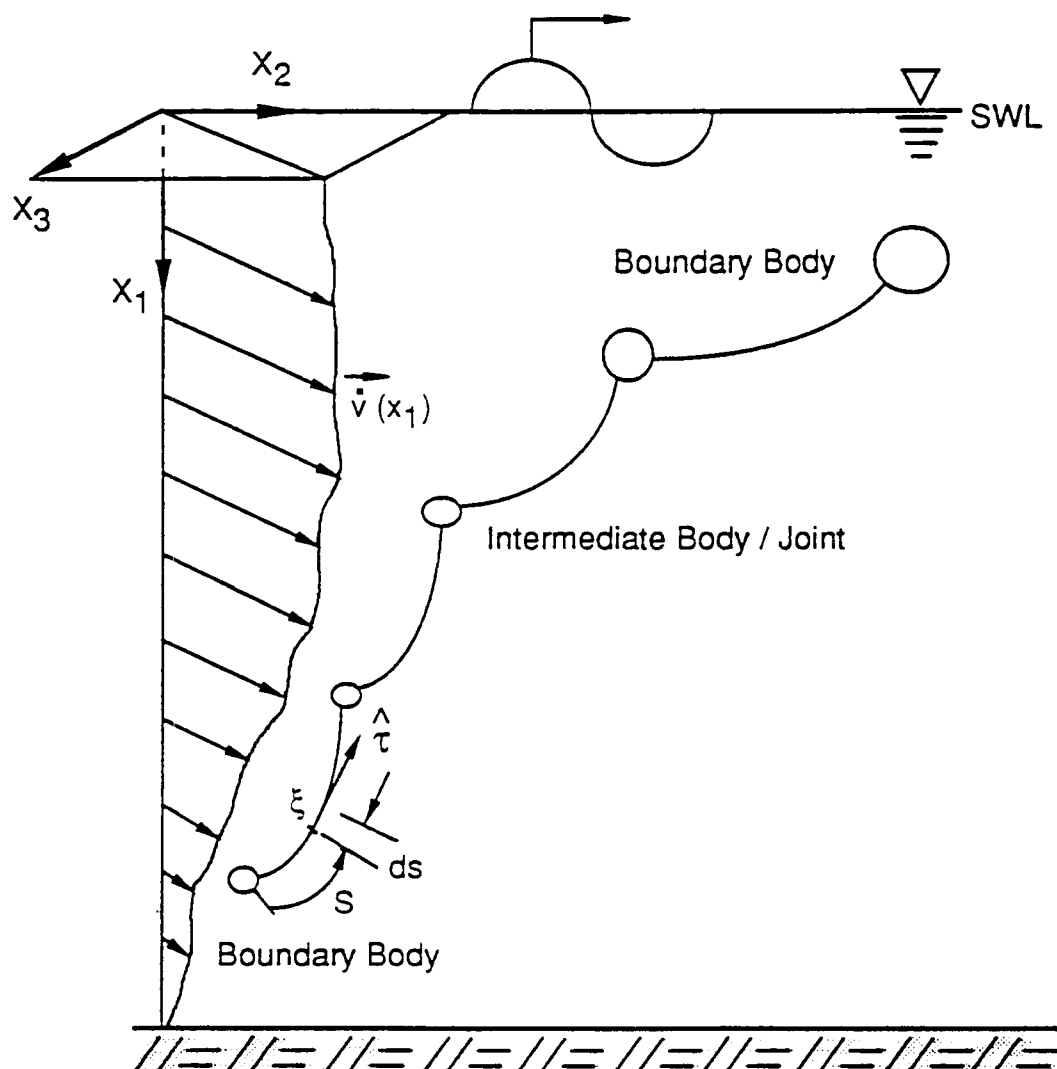
Figure 2.1 General Definition Sketch

2.1 Basic Assumptions

The following assumptions are made to mathematically model the cable-body

system:

1) The cable is treated as a slender, flexible circular cylinder. Thus, the

    calculation of the hydrodynamic forces by the Morison equation is valid.

2) The cable segment may be curved in three dimensions.

3) The cable is subject to uniaxial stress with no flexure, shear or torsion.

4) Nonlinear elastic behavior of the cable material is assumed with a tension-

    strain relation of the form

$$\epsilon = \sum_{n=0}^{3} a_n \, T^n$$

(2.1.1)

where ϵ is the cable stain, T is the magnitude of cable tension and a_n are

constants which describe the material characteristics. For a linear elastic

cable material with modulus of elasticity E and cross-sectional area A,

$a_1 = 1/EA$, $a_0 = a_2 = a_3 = 0.0$. For an inextensible cable material,

$a_0 = a_1 = a_2 = a_3 = 0.0$.

5) Only small elastic strains of the cable are considered.

6) Mass is conserved and the density of material does not change upon

    stretching. Thus, for a solid circular section the stretched cable diameter

    may be related to the unstretched cable diameter by

$$\rho \frac{\pi D_0^2}{4} \times 1 = \rho \frac{\pi D^2}{4} \times (1 + \epsilon)$$

therefore

$$\therefore \qquad D = \frac{D_0}{(1+\epsilon)^{\frac{1}{2}}} \qquad\qquad (2.1.2)$$

where D_0 is the unstretched cable diameter, D is the stretched cable diameter, and ϵ is the elastic strain.

7) Hydrodynamic drag and inertia forces on the slender cable are taken from the relative velocity form of the Morison equation. (Sarpkaya and Isaacson, 1981)

8) The drag coefficients $C_D{}^t$ and $C_D{}^n$ in the Morison equation are Reynolds' number dependent and also vary with relative roughness of the cable. In this study, they are taken as constant values.

9) In this study, intermediate and boundary bodies are assumed to be small enough that the Morison equation is applicable and only translational degrees-of-freedom (surge, sway and heave) of the bodies are considered. The enhancement of buoy treatment to include different buoy models and to consider buoy rotational degrees of freedom (pitch,roll and yaw) is under a separate study.

2.2 Basic Relationships

Let $\vec{r}$ be the position vector of the material point at ξ on the cable segment

$$\vec{r} = X_i \, \vec{e_i} \qquad\qquad i = 1,2,\dots,N$$

(2.2.1)

where X_i is the coordinate of point ξ, $\vec{e_i}$ the unit base vectors of cartesian space and N the dimension (2 or 3) of the problem. The summation convention on repeated indices is invoked.

The unit vector tangent to the cable segment $\vec{\tau}$ can then be obtained by differentiating the position vector with respect to the stretched arc length of the cable

$$\vec{\tau} = \frac{\partial \vec{r}}{\partial s} = \frac{\partial X_i}{\partial s} \, \vec{e_i} = \phi_i \, \vec{e_i}$$

(2.2.2)

where ϕ_i is the direction cosines of the cable segment at point ξ.

Let $\vec{q}$ be a relative velocity vector in cartesian space

$$\vec{q} = q_i \, \vec{e_i} \qquad\qquad i = 1,2,\dots,N$$

(2.2.3a)

Then, the tangent component of $\vec{q}$ can be calculated by

$$\vec{q^t} = (\vec{q} \cdot \vec{\tau}) \, \vec{\tau}$$
$$= (q_k \, \phi_k) \, \phi_i \vec{e_i}$$
$$= (\phi_i \, \phi_k q_k) \, \vec{e_i}$$

(2.2.3b)

The ith component of $\vec{q}^{\,t}$ in cartesian space is

$$q_i^{\,t} = \phi_i\,\phi_k\,q_k$$

<div align="right">(2.2.3c)</div>

and the magnitude of $\vec{q}^{\,t}$ is

<div align="right">(2.23d)</div>

$$q^{\,t} = |\,\vec{q}^{\,t}\,| = \sqrt{q_i^{\,t}\,q_i^{\,t}}$$

The normal component of $\vec{q}$ may be found according to

$$
\begin{aligned}
\vec{q}^{\,n} &= \vec{q} - \vec{q}^{\,t} \\
&= q_i\,\vec{e}_i - (q_k\,\phi_k\,\phi_i)\,\vec{e}_i \\
&= (q_i - \phi_i\,\phi_k\,q_k)\,\vec{e}_i
\end{aligned}
$$

<div align="right">(2.2.3e)</div>

The ith component of $\vec{q}^{\,n}$ in cartesian space is thus

<div align="right">(2.2.3f)</div>

$$q_i^{\,n} = q_i - \phi_i\,\phi_k\,q_k$$

and the magnitude of $\vec{q}^{\,n}$ is

<div align="right">(2.2.3g)</div>

$$q^{\,n} = |\,\vec{q}^{\,n}\,| = \sqrt{q_i^{\,n}\,q_i^{\,n}}$$

Tension $\vec{T}$ has the direction of $\vec{\tau}$ and has magnitude T, thus

$$\vec{T} = T\,\vec{\tau}$$

<div align="right">(2.2.4)</div>

Alternatively,

$$\vec{T} = T_i\,\vec{e}_i \qquad\qquad i = 1,2,\dots,N$$

<div align="right">(2.2.5)</div>

therefore,

$$T = (T_i \ T_i)^{\frac{1}{2}}$$

(2.2.6)

Also,

(2.2.7)

$$T_i = T \ \phi_i$$

Substituting (2.2.7) into (2.2.6), one obtains the familiar constraint on direction cosines

$$\{\phi_i \ \phi_i\}^{\frac{1}{2}} = 1$$

(2.2.8)

Assuming small strain, one can relate the stretched cable differential arc length, dS, to the unstretched cable differential arc length, dS_0, by

$$\frac{\partial S}{\partial S_0} = 1 + \epsilon$$

(2.2.9)

2.3 Loads

In addition to dead loads due to gravity, a submerged cable system is subject to environmental loadings from buoyancy, currents ,waves, tides and a variety of live loads peculiar to its application.

Gravity and Buoyancy

Assuming a completely submerged cable, both gravity and buoyancy forces are

uniformly distributed along the arc length of the cable segment. Let $\vec{W}_B$ represents the buoyant weight per unit length of the unstretched cable. Then

$$\vec{W}_B = W_B \, \vec{e}_3 \quad , \qquad W_B = (m - \rho A_0) \, g \qquad (2.3.1)$$

where m is the mass of unstretched cable per unit length, A_0 the cross-sectional area of the unstretched cable, ρ the fluid density and g the acceleration of gravity.

Fluid Drag Force

By the independence principle for drag on a slender inclined cylinder using the relative velocity form of the Morison equation (Sarpkaya and Isaacson, 1981), one can write the drag force per unit length of unstretched cable as

$$\vec{F}_{D0} = \frac{1}{2}\rho D_0 C_D^n |\vec{q}^n| \vec{q}^n + \frac{1}{2}\rho \pi D_0 C_D^t |\vec{q}^t| \vec{q}^t \qquad (2.3.2)$$

where ρ is the fluid density, D_0 the diameter of unstretched cable, C_D^n the normal drag coefficient, C_D^t the tangential drag coefficient, $\vec{q}^n$ the normal component of relative velocity vector, $\vec{q}^t$ the tangential component of relative velocity vector. The terms $|\vec{q}^n|$ and $|\vec{q}^t|$ denote the magnitudes of $\vec{q}^n$ and $\vec{q}^t$, respectively. The relative velocity is defined by

$$\vec{q} = \vec{u} + \vec{v} - \dot{\vec{X}} \qquad (2.3.3)$$

where $\vec{u}$ is the wave induced water particle velocity vector, $\vec{v}$ the current induced water particle velocity and $\dot{\vec{X}}$ the cable velocity vector.

Using the relationships of (2.2.3a) through (2.2.3g), one can write Eq.(2.3.2) in the component form as

$$F_{DOi} = \alpha_1 \, q^n q_i^n + \alpha_2 \, q^t q_i^t \qquad\qquad i = 1,2,\ldots,N \qquad (2.3.4a)$$

where

$$\alpha_1 = 0.5\rho D_0 C_D^n \qquad\qquad (2.3.4b)$$

$$\alpha_2 = 0.5\rho D_0 \pi C_D^t \qquad\qquad (2.3.4c)$$

$$q_i^t = \phi_i \, \phi_k \, q_k \qquad\qquad (2.3.4d)$$

$$q_i^n = q_i - q_i^t = q_i - \phi_i\phi_k q_k \qquad\qquad (2.3.4e)$$

$$q^t = \sqrt{q_k^t \, q_k^t} \qquad\qquad (2.3.4f)$$

$$q^n = \sqrt{q_k^n \, q_k^n} \qquad\qquad (2.3.4g)$$

The drag force per unit length of stretched cable $\overline{F}_D$ can be related to the drag force per unit length of unstretched cable $\overline{F}_{DO}$ by replacing D_0 by D in Eq.(2.3.2) and using the relationship (2.1.2).

$$\overline{F}_D = \frac{\overline{F}_{DO}}{(1+\epsilon)^{\frac{1}{2}}} \qquad\qquad (2.3.5)$$

Fluid Inertia Force

The fluid inertia force is that due to both the relative normal acceleration of the cable and to the pressure gradient of the oscillatory fluid flow. (Sarpkaya and Isaacson, 1981, Chakrabarti, 1987). The fluid inertia force per unit unstretched cable length can be written as

$$\overline{F}_{IO} = \frac{\pi D_0^2}{4}\rho \ (C_A+1) \ \overline{\ddot{u}^n} - \frac{\pi D_0^2}{4}\rho \ C_A\overline{\ddot{X}^n} \tag{2.3.6}$$

where D_0 is the diameter of unstretched cable, ρ the fluid density, C_A the added mass coefficient, $\overline{\ddot{u}^n}$ the normal component of wave induced water particle acceleration and $\overline{\ddot{X}^n}$ the normal component of cable acceleration. The current induced water particle acceleration is taken as zero. The first term of is due to the pressure gradient of the oscillatory fluid flow. The second term is attributed to the cable accelerating in still water.

Eq.(2.3.6) may be given in component form by

$$F_{IOi} = \alpha_3 \ \ddot{u}_i^n - \alpha_4 \ \ddot{X}_i^n \qquad i = 1,2,...,N \tag{2.3.7a}$$

where

$$\alpha_3 = \rho \ A_0 \ (C_A+1) \tag{2.3.7b}$$

$$\alpha_4 = \rho \ A_0 \ C_A \tag{2.3.7c}$$

$$\ddot{u}_i^n = \ddot{u}_i - \phi_i\phi_k\ddot{u}_k \tag{2.3.7d}$$

$$\ddot{X}_i^n = \ddot{X}_i - \phi_i\phi_k\ddot{X}_k \tag{2.3.7e}$$

Concentrated Loads and Body Excitations

To permit some versatility in loading, provision is made for the use of both concentrated loads and body excitations. The concentrated loads, both time dependent and time invariant, may be applied in arbitrary directions at the "joints" within the cable scope. Body motions may be prescribed only at boundary points. Both concentrated loads and body motion may be specified as sinusoidal functions or as discretized time histories.

2.4 Governing Equations

2.4.1 Kinematic Equations

From Eq.(2.2.2), the cartesian coordinates X_i of the cable point ξ are related to the direction cosines ϕ_i by

$$\frac{\partial X_i}{\partial S} = \phi_i \qquad\qquad i = 1,2,...,N \qquad (2.4.1)$$

where X_i is the coordinate of cable material at point ξ, S the stretched cable length and ϕ_i the direction cosines of cable differential arc length, dS, at point ξ.

The Eq.(2.4.1) can be expressed in term of the unstretched cable length S_0 by using the relationship (2.2.9).

$$\frac{\partial X_i}{\partial S_0} = (1 + \epsilon) \phi_i$$

$$(2.4.2)$$

$$i = 1,2,...,N$$

where ϵ is the strain of the cable differential arc length,dS,at point ξ.

2.4.2 Dynamic Equilibrium Equations of Cable Segment

At a general point ξ on a cable, a stretched differential length,dS, can be isolated as a free body as shown in Fig.2.2. The external forces acting on that free body are the buoyant weight, the drag force and added inertia forces due to relative motion through the fluid. These external forces are balanced by the variation in end point tensions over the differential length dS and the inertia force due to the cable acceleration. The balance of the forces at a point ξ of the stretched cable may be written in a vector form (Ablow and Schechter, 1983)

$$\frac{\partial}{\partial S}\,\overline{T} + \frac{1}{(1+\epsilon)}\,\overline{W}_B + \overline{F}_D + \frac{\overline{F}_{IO}}{(1+\epsilon)} + \frac{\overline{I}}{(1+\epsilon)} = 0 \tag{2.4.3}$$

where the independent variable S is the arc length along the stretched cable, $\overline{T}$ is the tension, $\overline{W}_B$ is the buoyant weight per unit length of unstretched cable, $\overline{F}_D$ is the hydrodynamic drag force per unit stretched length and $\overline{F}_{IO}$ is the hydrodynamic inertia force per unit unstretched length, and $\overline{I}$ is the d'Alembert force due to the cable acceleration per unit unstretched length and ϵ is the strain.

Expressing (2.4.3) in term of unstretched cable length and using the relationship (2.3.5), one obtains

$$\frac{\partial \overline{T}}{\partial S_0} = (1+\epsilon)\frac{\partial \overline{T}}{\partial S} = -m\,\overline{\ddot{X}}_i - \overline{F}_{IO} - (1+\epsilon)^{\frac{1}{2}}\,\overline{F}_{DO} - \overline{W}_B \tag{2.4.4}$$

where m is the mass density of the cable per unit unstretched length and $\overline{\ddot{X}}_i$ is the acceleration vector of the cable at point ξ.

This vector dynamic equation can be written in component form in cartesian space as

$$\frac{\partial T_i}{\partial S_0} = -m\,\ddot{X}_i - F_{IOi} - (1+\epsilon)^{\frac{1}{2}}\,F_{DOi} - W_B\,\delta_{1i} \tag{2.4.5}$$

where δ_{1i} is the Kronecker delta ($\delta_{1i}=1$, if i=1, otherwise $\delta_{1i}=0$). One should note that all the terms on the right hand side of the equilibrium equation (2.4.5) are now expressed in term of the unstretched cable length.
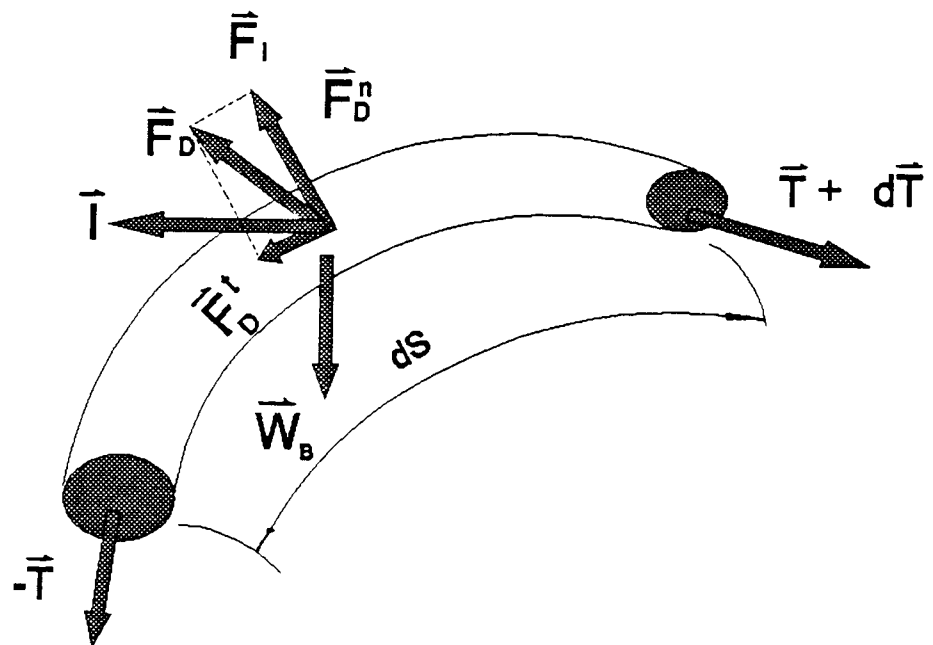
Figure 2.2 Free Body Diagram of Cable Segment

The gradient of the auxiliary variables T_i in Eq.(2.4.5) needs to be expressed in terms of the fundamental variables ϕ_i. Taking a derivative of Eq.(2.2.7) with respect to S_0, one obtains

$$\frac{\partial \phi_i}{\partial S_0} = \frac{1}{T}\frac{\partial T_i}{\partial S_0} - \frac{\phi_i}{T}\frac{\partial T}{\partial S_0}$$

(2.4.6)

From (2.2.6)

$$\frac{\partial T}{\partial S_0} = \frac{1}{T} T_k \frac{\partial T_k}{\partial S_0} = \phi_k \frac{\partial T_k}{\partial S_0}$$

(2.4.7)

Combining (2.4.6) and (2.4.7), one obtains

$$\frac{\partial \phi_i}{\partial S_0} = \frac{1}{T}\frac{\partial T_k}{\partial S_0}(\delta_{ik} - \phi_i \phi_k)$$

(2.4.8)

Substituting Eq.(2.4.5) into (2.4.8), obtains

$$\frac{\partial \phi_i}{\partial S_0} = \frac{1}{T}(\delta_{ik} - \phi_i \phi_k)\left(m \ddot{X}_k - F_{I0k} - (1+\epsilon)^{\frac{1}{2}} F_{D0k} - W_B \delta_{1k}\right)$$

(2.4.9)

$$i, k = 1,2,\ldots,N$$

It should be noted, however, that not all ϕ_i are independent because of constraint (2.2.8).

To obtain a governing equation for the fundamental variable T, Substitute Eq.(2.4.5) into (2.4.7)

$$\frac{\partial T}{\partial S_0} = \phi_k \left(m \ddot{X}_k - F_{I0k} - (1+\epsilon)^{\frac{1}{2}} F_{D0k} - W_B \delta_{1k}\right)$$

(2.4.10)

$$k = 1,2,\ldots,N$$

Use this equation to replace one of Eqs.(2.4.9) since the ϕ_i are not independent. Also, one should note that potential singularities, i.e. $T=0$, are present in Eqs.(2.4.9) only, but not in Eqs.(2.4.2) or (2.4.10)

2.5 Boundary Conditions

In N dimensional space Eqs.(2.4.9),(2.4.12) and (2.4.10) constitute 2N dynamic ordinary differential equations of the second order for the 2N unknowns of N coordinates X_i, N-1 direction cosines ϕ_j and one tension magnitude T. The independent variables are the unstretched cable arc length coordinate S_0 and time t. Thus, 2N boundary conditions at the two ends need to be specified at all times.

The boundary conditions for the problem may be generalized as two types: 1) kinematic boundary conditions, 2) force boundary conditions.

2.5.1 Kinematic Boundary Conditions

The kinematic boundary conditions can be expressed by either specified velocity functions or specified coordinate functions at boundary ends of the system. These functions may be defined as zero values, discretized time-history functions or sinusoid functions.

For the specified velocity function, the boundary condition may be expressed by

$$\dot{X}_i(t) = \dot{X}_i^s(t) \tag{2.5.1}$$

where $\dot{X}_i^s(t)$ denotes specified velocity component at boundary at time t.

If the coordinate function is specified, The specified coordinates $X_i^s(t)$ may be converted to the specified velocities according to the following finite difference approximation

$$\dot{X}_i^s(t) = \frac{\partial X_i^s}{\partial t} = \frac{X_i^s - X_i^p}{\alpha \Delta t} - \gamma \dot{X}_i^p$$

(2.5.2)

Here "p" denotes specified value at previous time step. The parameters α and γ are constants ($\alpha = 0.5$, $\gamma = 1.0$). See Section 2.6.1 for elaboration.

Hinged or Moving Boundary Conditions

If $\dot{X}_i^s(t) \equiv 0$ or $X_i^s(t) = $ constant, Eqs.(2.5.1) express a hinged boundary condition. Otherwise they define a moving boundary condition.

Payout Boundary Conditions

There are two types of payout operations: passively controlled payout and actively controlled payout. For passively controlled payout, the cable tension magnitude T is constant at the particle detaching from the shipboard canister or reel with the cable velocity at the payout point undetermined. For actively controlled payout, which is assumed for the AOR project, the payout rate relative to the moving ship is specified rather than the tension magnitude. The cable velocity vector at the payout point is

$$\vec{\dot{X}^s}(t) = \vec{V}_s + V_p \vec{\tau}$$

(2.5.3)

where $\vec{V}_s$ and V_p are the ship speed vector and the cable payout rate relative to the moving ship, respectively, and $\vec{\tau}$ is the unit tangent vector (with unknown direction) of the cable at the payout point. The cable velocity components at the payout point can

then be written as

$$\dot{X}_i^s(t) = V_{si} + V_p \, \phi_i \qquad (2.5.4)$$

where V_{si} is the ith component of the ship speed, V_p is the payout rate relative to the

moving ship and ϕ_i is the unknown ith direction cosine of the cable at the payout

point.

Compatibility Conditions at Intermediate Bodies

In order to continue the numerical integration across an intermediate body, the

following kinematic compatibility conditions are required

$$(\dot{X}_i)_{cable} = (\dot{X}_i)_{body} \qquad (2.5.5)$$

2.5.2 Force Boundary Conditions

The force boundary conditions include intermediate and boundary body

boundary conditions, the free end boundary conditions and cable/ocean-bottom contact

boundary conditions.

Intermediate and Boundary Body Boundary Conditions

By assumption 9) the intermediate bodies are small. Therefore, the Morison

equation can be used to calculate hydrodynamic forces. Fig 2.3 shows a isolated free

body diagram for an intermediate body. The external forces acting on the free body

are buoyant weight $\vec{W}$ of body, drag and added inertia forces $\vec{F}$ due to relative

motion through fluid, constant and time-dependent concentrated loads, $\vec{P}_0$ and $\vec{P}$ (t),

and spring reaction force $\vec{R}$. These external forces are balanced by the change in the

tensions $^b\vec{T}$ and $^a\vec{T}$ at connection points and by the d'Alembert force $\vec{I}$ due to body
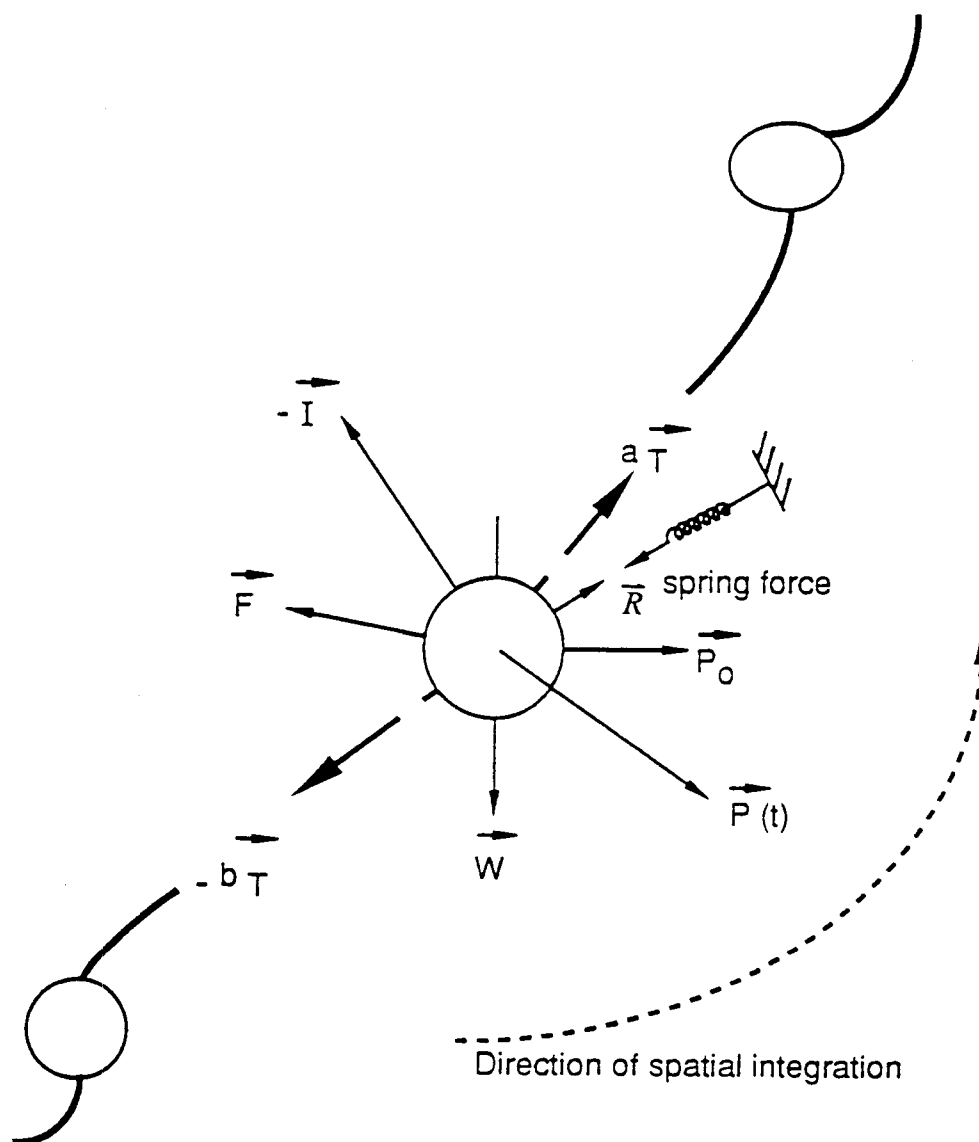
Figure 2.3 Free Body Diagram of Intermediate Body

acceleration. The equilibrium equations of dynamic forces in N dimension on the free body corresponding to N translational degrees-of-freedom can be written as

$$-(M + \rho \, C_A \, V) \, \ddot{X}_i + (C_A + 1) \, \rho \, V \, \ddot{u}_i + \beta \, q \, q_i + P_i(t) + P_{0i}$$
$$+ \, W \, \delta_{1i} - k \, (X_i - X_{oi}) - {}^b\phi_i \, {}^bT + {}^a\phi_i \, {}^aT = 0 \qquad (2.5.6)$$

$$i = 1, 2, ..., N$$

where

M	=	mass of the intermediate body.
W	=	buoyant weight of the intermediate body,
V	=	volume of the intermediate body,
C_A	=	added mass coefficient,
q_i	=	ith component of relative velocity,
q	=	magnitude of relative velocity
β	=	$0.5 \rho A_0 C_D$,
A_0	=	drag area of the intermediate body,
C_D	=	drag coefficient of the intermediate body,
k	=	stiffness constant of the spring attached to the body,
X_{0i}	=	reference coordinates where the spring is unstretched,
$P_i(t)$	=	time-dependent concentrated load,
P_{oi}	=	constant concentrated load,
${}^b\phi_i, {}^a\phi_i$	=	the direction cosines at the connection points "before" and "after" the body,
${}^bT, {}^aT$	=	the tension at the connection points "before" and "after" the body.

In Eq.(2.5.6) rotational degrees of freedom and corresponding restoring moments have been ignored.

The equilibrium equations for a boundary body are identical to those for an intermediate body except that there is only one cable tension force acting on the body. Thus, similar equilibrium equations to Eq.(2.5.6) can be derived for a boundary body

$$
\begin{aligned}
& - (M + \rho\ C_A\ V)\ \ddot{X}_i + (C_A + 1)\ \rho V\ \ddot{u}_i + \beta\ q\ q_i \\
& + P_i(t) + P_{0i} + W\ \delta_{1i} - k\ (X_i - X_{0i}) \pm \phi_i T = 0
\end{aligned}
\tag{2.5.7}
$$

$$
i = 1,2,\ldots,N
$$

The selection of the sign for the last term of (2.5.7) depends up on where the boundary body is located. The positive sign should be chosen for the body located at the starting end of the spatial integration, the negative sign for the body located at the terminal end of the spatial integration.

Free End Boundary Conditions

At a free end of a cable a singularity, i.e. $T=0$, exists at the free end. In order to avoid the singularity, one may consider the boundary condition to be applied at point P, a short distance Δ from the free end. Assuming the cable segment from the free end to the point P is a straight-line (which implies zero curvature $\partial\phi_i/\partial S_0 = 0$) and integrating the dynamic equilibrium equation for tension magnitude (2.4.6), one may obtain

$$
\phi_i\ T = \frac{\partial T_i}{\partial S_0}\ \Delta \qquad\qquad i = 1,2,\ldots N
\tag{2.5.8}
$$

Substituting Eq.(2.4.5) into (2.5.8), one obtains a simplified dynamic equilibrium

equations of this short cable segment in the component form as

$$\left(-m \; \ddot{X_i} \; + \; F_{I0i} \; + \; (1+\epsilon)^{\frac{1}{2}} \; F_{D0i} \; + \; W_B \delta_{1i}\right) \Delta \; - \; \phi_i \; T \; = \; 0$$

(2.5.9)

$$i = 1,2,\ldots,N$$

where m is the mass density per unit unstretched cable length, $\ddot{X_i}$ the ith component of the average acceleration of cable segment, F_{I0i} and F_{D0i}, the ith component of the average hydrodynamic inertia and drag force per unit unstretched cable length respectively, W_B the buoyant weight per unit unstretched cable length, Δ the distance from free end to the point P, ϕ_i the direction cosines of the short cable segment and T the tension magnitude at the point P.

Slack-Cable/Ocean-Bottom Contact Boundary Conditions

The boundary conditions at the touchdown point may depend upon the different payout operation conditions. If the payout rate is less than the ship speed, the cable will tend to be dragged along the ocean bottom. The frictional resistance between the ocean floor and the cable laying on the bottom produce a non-zero tension magnitude within the cable at the touchdown point. Thus, the cable segment at the touchdown point may be expected to be tangent to the ocean floor. However, in a the realistic cable deployment operation using actively controlled payout, a payout rate greater than the ship speed is usually specified in order to place more cable between the two points on the bottom than the straight-line distance between those two points. This generates a slack cable deposited on the bottom which is desirable because of smaller tensions in the installed cable, no dragging, less chance of snags and smaller suspensions over irregular ocean bottoms. Because the cable is not dragged along and can not penetrate

through the ocean floor, one may write the boundary conditions as

$$\dot{X}_i = 0 \qquad\qquad i=1,2,\ldots,N \qquad\qquad (2.5.10)$$

where $\dot{X}_i$ is the cable velocity component at the touchdown point.

This is subject to the constraint

$$X_1(S_u) = D \qquad\qquad (2.5.11)$$

where $X_1(S_u)$ is the X_1 coordinate of the touchdown point at an undetermined unstretched cable length of S_u and D is the depth to the ocean floor.

Since the tension magnitude at the touchdown point is zero, the cable at the touchdown point may be regarded as a free end. Thus, one obtains the boundary condition at the point P, a short distance from the touchdown point, in the same form as the free end boundary conditions (2.5.9) except that the velocity at the free end is zero and is subject to the constraint (2.5.11). With such a boundary condition specified, a kink rather than a tangent cable segment may be expected at the touchdown point.

2.6 The Quasi-static Governing Equations and Boundary Conditions

The kinematic equations (2.4.2) and the dynamic equilibrium equations (2.4.9) and (2.4.10) of cable segments, with boundary conditions detailed in Section 2.5, constitute a combined boundary-value and initial-value problem because of the time evolution.

2.6.1 Implicit Integration Scheme

In order to convert from a combined initial-value and boundary-value problem to a discrete two-point boundary-value problem at each time, a stable implicit integration scheme based on a Newmark-like formula is introduced (Leonard,1988). The dynamic problem may then be treated as an equivalent static problem at each time instant t.

Assume the solution at time t^p is known. Let Δt be the time step to the later unknown solution at time $t = t^p + \Delta t$, The time derivatives of the dependent variables may be approximated by

$$a_i = \frac{\partial \dot{X}_i}{\partial t} = \frac{\dot{X}_i - \dot{X}_i^p}{\alpha \Delta t} - \gamma a_i^p \tag{2.6.1a}$$

$$\eta_i = \frac{\partial \phi_i}{\partial t} = \frac{\phi_i - \phi_i^p}{\alpha \Delta t} - \gamma \eta_i^p \tag{2.6.1b}$$

$$\xi = \frac{\partial T}{\partial t} = \frac{T - T^p}{\alpha \Delta t} - \gamma \xi^p \tag{2.6.1c}$$

$$\dot{X}_i = \frac{\partial X_i}{\partial t} = \frac{X_i - X_i^p}{\alpha \Delta t} - \gamma \dot{X}_i^p \tag{2.6.1d}$$

where the superscript, "p", indicates known values at a prior time step. The parameters α and γ are integration constants. The parameter γ can be related to α by $\gamma = (1-\alpha)/\alpha$. If $\alpha = 1$, and $\gamma = 0$, Eqs.(2.6.1) reduce to the backward difference formulae used in KBLDYN (Chiou, 1989). If $\alpha = 0.5$ and $\gamma = 1.0$, (2.6.1) represent an implicit average acceleration method which is a special case of Newmark's method

(Clough and Penzien,1975).

From (2.6.1d), one obtain the expression for coordinates

$$X_i = X_i^p + \alpha \Delta t \ (\dot{X}_i + \gamma \dot{X}_i^p)$$

(2.6.2)

The above implicit integration scheme will be stable for time steps much larger than those permitted by an explicit method. Moreover, the numerical damping to the solution will be greatly reduced. This feature will be examined in the first example problem of Chapter 4.

2.6.2 Transformation of Kinematic Equations to Phase Space

In order to balance the accuracy of the kinematic and dynamic equations when discretized in time, the kinematic equations need to be transformed into phase space and an auxiliary variable of cable velocity introduced. Taking the time derivative of Eq.(2.4.2), interchanging the order of differentiation and using the chain rule of differentiation, one obtains kinematic compatibility equations in the form

$$\frac{\partial}{\partial t} \left[\frac{\partial X_i}{\partial S_0} \right] = \frac{\partial}{\partial S_0} \left[\frac{\partial X_i}{\partial t} \right] = \frac{\partial \dot{X}_i}{\partial S_0}$$

(2.6.3)

thus

$$\frac{\partial \dot{X}_i}{\partial S_0} = (1 + \epsilon) \ \frac{\partial \phi_i}{\partial t} + \frac{\partial \epsilon}{\partial t} \ \phi_i$$

(2.6.4)

or

$$\frac{\partial \dot{X}_i}{\partial S_0} = (1 + \epsilon) \ \frac{\partial \phi_i}{\partial t} + \frac{\partial \epsilon}{\partial T} \ \frac{\partial T}{\partial t} \ \phi_i$$

(2.6.5)

$$i = 1,2,...,N$$

where $\dot{X}_i$ is the ith velocity component of the cable at point ξ, ϵ the strain of cable at point ξ, ϕ_i the direction cosines of cable at point ξ and T the tension magnitude at point ξ.

2.6.3 Quasi-Static Governing Equations

Replacing time derivative terms of the dependent variables $\dot{X}_i$, ϕ_i and T in Eqs. (2.6.5), (2.4.9) and (2.4.10) by Eqs. (2.6.1a) through (2.6.1d), one obtains the quasi-static governing equations of a cable segment as

$$\frac{d\dot{X}_i}{dS_0} = (1+\epsilon) \, \eta_i + \frac{\partial \epsilon}{\partial t} \, \xi \, \phi_i = f_i(\phi_k, T) \tag{2.6.6a}$$

$$\frac{d\phi_j}{dS_0} = \frac{1}{T}(\delta_{jk} - \phi_j \phi_k) \left(ma_k - F_{I0k} - (1+\epsilon)^{\frac{1}{2}} F_{D0k} - W_B \delta_{1k} \right) = g_j(\dot{X}_k, \phi_k, T) \tag{2.6.6b}$$

$$\frac{dT}{dS_0} = \phi_k \left(ma_k - F_{I0k} - (1+\epsilon)^{\frac{1}{2}} F_{D0k} - W_B \delta_{1k} \right) = h(\dot{X}_k, \phi_k, T) \tag{2.6.6c}$$

$$i, k = 1,2,...,N; \, j \in J$$

where f_i, g_j, h denote functions on the right hand of Eqs. (2.6.6a) through (2.6.6c) respectively. The dependent variables are

$$\{Y\} = \begin{Bmatrix} \dot{X}_i \\ \phi_j \\ T \end{Bmatrix} \tag{2.6.6d}$$

$$i=1,2,...,N; \, j \in J$$

subject to the constraint

$$\phi_e = \pm(1-\phi_j\phi_j)^{\frac{1}{2}} \qquad\qquad j \in J$$

<div align="right">(2.6.6e)</div>

where ϕ_e is the direction cosine to be eliminated from the set of dependent variables. The term J denote the set of numbers from 1 to N exclusive of e and may be expressed as

$$J=\{1,2,...,N \setminus e\}$$

<div align="right">(2.6.6f)</div>

2.6.4 Quasi-static Force Boundary Conditions

Replacing the acceleration term $\ddot{X}_i$ in Eqs.(2.5.6),(2.5.7) and (2.5.9) for intermediate body, boundary body and cable free end boundary conditions by the finite difference expression (2.6.1a), one obtains the quasi-static force boundary conditions as follows:

Intermediate Boundary Conditions

$$- (M+\rho C_A V)a_i + (C_A+1)\rho V\ddot{u}_i + \beta qq_i + P_i(t) + P_{0i}$$
$$+ W\delta_{1i} - k(X_i-X_{0i}) -^b\phi_i^b T +^a\phi_i^a T = 0$$

<div align="right">(2.6.7)</div>

$$i = 1,2,...,N$$

Boundary Body Boundary Conditions

$$- (M+\rho C_A V)a_i + (C_A+1)\rho V\ddot{u}_i + \beta qq_i + P_i(t) + P_{0i}$$
$$+ W\delta_{1i} - k(X_i-X_{0i}) \pm \phi_i T = I_i(\dot{X}_k,\phi_l,T) = 0$$

<div align="right">(2.6.8)</div>

$$i = 1,2,...,N$$

Cable Free End Boundary Conditions

$$\left(-m\ a_i\ +\ F_{IOi}\ +\ (1+\epsilon)^{\frac{1}{2}}\ F_{DOi}\ +\ W_B\delta_{1i}\right)\ \Delta\ -\ \phi_i\ T\ =\ L_i(\dot{X}_k,\phi_l,T)\ =\ 0 \tag{2.6.9}$$

$$i=1,2,\ldots,N$$

In this chapter, 2N governing equations and corresponding boundary conditions for the dynamic problem of a cable/lumped-body system have been derived and specified. In the next chapter, a solution algorithm will be presented to solve the problem at discrete times Δt apart.

3.0 NUMERICAL METHODS

The implicit time integration method described in section 2.6 allows the treatment of a dynamic problem as an equivalent static problem at each time instant. Thus the nonlinear dynamic problem presented in Chapter 2 poses a two-point boundary-value problem in the spatial coordinate at each time. The traditional shooting method (Press et al.,1986) for solving this problem is not to be successful because of the nonlinearities and discontinuities at the intermediate bodies (Ablow and Schechter,1983).

The adopted computational scheme is to first transform the nonlinear two-point boundary value problem into a quasi-linearized two-point boundary value problem to be solved iteratively. The quasi-linearized two-point boundary value problem is then further decomposed into a set of quasi-linear initial-value problems in the spatial coordinate so the numerical integration can be performed along the cable from one end to the other. In solving initial-value problems difficulties may arise during the direct numerical integration of partial solutions. Since the solutions are of the exponential type, the extraneous growth of the solution profiles (partial solutions) over the long integration path may lead to illconditioned terminal boundary conditions and result in larger and larger errors in the sequence of linear two-point boundary-value problems. To overcome this problem the suppression technique (Carter et al.,1969; Leonard,1969) may be applied. The suppression method consists of recombining the independent initial value problems (partial solutions) when necessary as the integration

proceeds. They are recombined in such a way that the components of the erroneous growing solutions at the point in question are eliminated. With this technique, the solutions are all of comparable magnitude when the integration process arrives at the terminal end of the cable. Whenever the partial solutions have become large compared with initial condition or previous solutions, the suppression is accomplished by requiring that linear combinations of the unsuppressed partial solutions satisfy the fictitious conditions. The fictitious conditions to be satisfied must be arbitrary, independent conditions which have small magnitudes compared with the partial solutions.

3.1 Newton-Raphson Quasi-Linearization

Assume a set of 2N nonlinear first-order differential equations

$$\left\{ \frac{dY_i}{dS} \right\} = \left\{ f_i(S, Y_j) \right\} \tag{3.1.1}$$

$$i, j = 1, 2, \ldots, 2N$$

with N nonlinear boundary conditions at boundary $S = 0$

$$\left\{ \bar{h}_k(\bar{Y}_j) \right\} = \{0\} \tag{3.1.2a}$$

$$k = 1, 2, \ldots, N$$

and N nonlinear boundary conditions at boundary $S = L_0$

$$\{\bar{\bar{h}}_k(\bar{\bar{Y}}_j)\} \ = \ \{0\}$$

$$(3.1.2b)$$

$$k=1,2,\ldots,N$$

where S is the independent variable (eg. cable arc length), $\{Y_j\}$ are the 2N dependent variables (e.g. velocity components, direction cosines and tension magnitude), $\{f_i(s, Y_j)\}$ are nonlinear functions of $\{Y_j\}$, and $\{\bar{h}_k(\bar{Y}_j)\}$ and $\{\bar{\bar{h}}_k(\bar{\bar{Y}}_j)\}$ are nonlinear functions of $\{\bar{Y}_j\}$ at S=0 and of $\{\bar{\bar{Y}}_j\}$ at $S=L_0$, respectively.

Let $\{Y_j^*\}$ denote a trial solution vector in the neighborhood of the true solution vector $\{Y_j\}$. The $\{\bar{Y}_j^*\}$ and $\{\bar{\bar{Y}}_j^*\}$ are corresponding boundary values of $\{Y_j^*\}$ at S=0, and $S=L_0$ respectively. In the following, asterisks will be used to indicate functions calculated from a trial solution. Expanding the nonlinear functions $\{f_i(s,Y_j)\}$, $\{\bar{h}_k(\bar{Y}_j)\}$, and $\{\bar{\bar{h}}_k(\bar{\bar{Y}}_j)\}$ in a truncated Taylor series up through first-order terms about $\{Y_j^*\}$, $\{\bar{Y}_j^*\}$ and $\{\bar{\bar{Y}}_j^*\}$, Eqs.(3.1.1),(3.1.2a) and (3.1.2b) may be written in the form (Chiou,1989).

$$\left\{\frac{dY_i}{ds}\right\} = \left[a_{ij}^*\right]\{Y_j\} + \{b_i^*\} \tag{3.1.3}$$

$$ij = 1,2,\ldots,2N$$

with boundary conditions at $S=0$

$$\left[\bar{c}_{kj}^*\right]\{\bar{Y}_j\} + \{\bar{d}_k^*\} = \{0\} \tag{3.1.4a}$$

$$k = 1,2,\ldots,N$$

and boundary conditions at $S=L_0$

$$\left[\bar{\bar{c}}_{kj}^*\right]\{\bar{\bar{Y}}_j\} + \{\bar{\bar{d}}_k^*\} = \{0\} \tag{3.1.4b}$$

$$k = 1,2,\ldots,N$$

where

$$\left[a_{ij}^*\right] = \left[J_{ij}^*\right] \tag{3.1.5a}$$

$$\{b_i^*\} = \{f_i^*(s,Y_j^*)\} - \left[J_{ij}^*\right]\{Y_j^*\} \tag{3.1.5b}$$

$$\left[\bar{c}_{kj}^*\right] = \left[\bar{J}_{kj}^*\right] \tag{3.1.5c}$$

$$\{\bar{d}_k^*\} = \{\bar{h}_k(\bar{Y}_j^*)\} - \left[\bar{J}_{kj}^*\right]\{\bar{Y}_j^*\} \tag{3.1.5d}$$

$$\left[\bar{\bar{c}}_{kj}^*\right] = \left[\bar{\bar{J}}_{kj}^*\right] \tag{3.1.5e}$$

$$\{\bar{\bar{d}}_k^\bullet\} = \{\bar{\bar{h}}_k^\bullet(\bar{\bar{Y}}_j^\bullet)\} - \left[\bar{\bar{J}}_{kj}^\bullet\right]\{\bar{\bar{Y}}_j^\bullet\} \qquad (3.1.5f)$$

In Eqs.(3.1.5), $[J_{ij}^\bullet]$, $[\bar{J}_{kj}^\bullet]$ and $[\bar{\bar{J}}_{kj}^\bullet]$ are the Jacobian matrices of governing

equations, initial boundary conditions and terminal boundary conditions, respectively.

Equation (3.1.3) with boundary conditions (3.1.4) and coefficients defined by Eqs.

(3.1.5) constitutes a linearized boundary-value problem for $\{Y_j\}$.

An iterative procedure can be applied to solve Eq.(3.1.3) for $\{Y_j\}$ in terms of

S and $\{Y_j^\bullet\}$. Starting with a set of trial solutions, further improved solutions are

obtained by successive iterations in Eqs. (3.1.5) with $\{Y_j^\bullet\}$, $\{\bar{Y}_j^\bullet\}$ and $\{\bar{\bar{Y}}_j^\bullet\}$

replaced by $\{Y_j\}$, $\{\bar{Y}_j^\bullet\}$ and $\{\bar{\bar{Y}}_j^\bullet\}$ generated by the previous iteration. The

iteration process continues until the difference between $\{Y_j\}$ and $\{Y_j^\bullet\}$ is less than a

stipulated error tolerance. A relative error at each integration point is calculated by

$$e = \sqrt{\sum \left(\frac{Y_i - Y_i^\bullet}{Y_i^\bullet}\right)^2} \qquad (3.1.6)$$

$$i = 1, 2, \ldots, 2N$$

3.2 Decomposition of Quasi-Linearized Boundary-Value Problem

A linear two-point boundary-value problem such as that posed by Eqs. (3.1.3) and (3.1.4) can be solved by first decomposing the problem into a set of initial-value problems and then recombining the solutions to each initial-value problem to satisfy all boundary conditions (Lee,1966; Leonard, 1979; Chiou and Leonard, 1990).

In general, the solution to each one of a linear set of 2N first-order differential equations can be considered as a linear combination of the solutions of (N+1) initial-value problems, hereafter called partial solutions. Assume the solutions to Eq (3.1.3) can be written as

$$\{Y_i\} = \{Y_i^0\} + [Y_{ik}] \{\zeta_k\}$$

$$(3.2.1)$$

$$i=1,2,...,2N; \ k=1,2,...,N$$

where $\{\zeta_k\}$ are undetermined parameters and $\{Y_i^0\}$ and $[Y_{ik}]$ are partial solutions associated with particular and homogeneous solutions, respectively, of Eq. (3.1.3). Substituting Eq. (3.2.1) into Eq. (3.1.3), one obtains a particular differential equation for $\{Y_i^0\}$ and N homogeneous differential equations for $[Y_{ik}]$ as

$$\left\{\frac{dY_i^0}{ds}\right\} = \left[a_{ij}^{\bullet}\right] \{Y_j^0\} + \{b_i^{\bullet}\} \qquad (3.2.2a)$$

and

$$\left\{\frac{dY_{ik}}{\partial s}\right\} = \left[a_{ij}^{\bullet}\right]\{Y_{jk}\} \tag{3.2.2b}$$

$$i, j = 1, 2, \ldots, 2N; \quad k = 1, 2, \ldots, N$$

To solve the decomposed linear boundary-value problem by a spatial integration along the independent variable, a set of initial values to Eqs (3.2.2a) and (3.2.2b) is required such that partial solutions can be obtained by numerical integration. Since the original problem is a boundary-value problem, the unknown values of dependent variables are located at both boundaries. Rather than use a set of blindly guessed initial values as in the shooting method (Press et al., 1986),it is always possible to obtain a set of initial values that satisfy the known boundary values. To obtain the initial values for the partial solutions, let $[\overline{c}_{kj}^{\bullet}]$ and $\{\overline{Y}_j\}$ in Eq. (3.1.4a) be partitioned as

$$\left[\overline{c}_{kj}^{\bullet}\right] = \left[{}^{I}\overline{c}_{kn}^{\bullet} \ {}^{II}\overline{c}_{kn}^{\bullet}\right] \tag{3.2.3a}$$

$$\{\overline{Y}_j\} = \left\{\begin{matrix} {}^{I}\overline{Y}_n \\ {}^{II}\overline{Y}_n \end{matrix}\right\} = \left[\begin{matrix} {}^{I}\overline{Y}_{nm} \\ {}^{II}\overline{Y}_{nm} \end{matrix}\right]\{\zeta_m\} + \left\{\begin{matrix} {}^{I}\overline{Y}_n^0 \\ {}^{II}\overline{Y}_n^0 \end{matrix}\right\} \tag{3.2.3b}$$

$$j = 1, 2, \ldots, 2N; \quad k, m, n = 1, 2, \ldots, N$$

where left superscripts, I and II, represent partition I and partition II, respectively.

Both $\{\overline{Y}_j\}$ and $[\overline{c}_{kj}^{\bullet}]$ are rearranged and partitioned such that $\{\overline{Y}_n\}$ represents the known initial values to the boundary-value problem posed by Eq. (3.1.3). The

unknown initial values of the partial solutions, $\{^{II}\bar{Y}^0_n\}$ and $\{^{II}\bar{Y}_{nm}\}$, to the initial-value

problem posed by Eqs. (3.2.2a) and (3.2.2b) may then be determined by substituting

Eqs. (3.2.3) into Eq. (3.1.8a) as

$$\{^{II}\bar{Y}^0_n\} = -\left[^{II}\overline{c^*_{kn}}\right]^{-1}\left[^I\overline{c^*_{kn}}\right]\{^I\bar{Y}^0_n\} - \left[^{II}\overline{c^*_{kn}}\right]^{-1}\{\bar{d}^*_n\}$$

(3.2.4a)

and

$$\left[^{II}\bar{Y}_{nm}\right] = -\left[^{II}\overline{c^*_{kn}}\right]^{-1}\left[^I\overline{c^*_{kn}}\right]\left[^I\bar{Y}_{nm}\right]$$

(3.2.4b)

Having defined (N+1) linearly independent initial-value problems, each of

which satisfies the actual boundary conditions at the starting end, numerical

integration may be performed to obtain the partial solutions at the terminal end. These

partial solutions at the terminal end are then used to determine the appropriate

coefficients, $\{\zeta_k\}$, in Eq.(3.2.1) for the linear combination of partial solutions. The

boundary conditions expressed by Eq. (3.1.4b) at the terminal end can be expressed

in terms of partial solutions as

$$\left[\bar{\bar{c}}^*_{kj}\right]\left\{\{\bar{\bar{Y}}^0_j\} + \left[\bar{\bar{Y}}_{jm}\right]\{\zeta_m\}\right\} + \{\bar{\bar{d}}^*_k\} = \{0\}$$

(3.2.5)

$$j=1, 2,..., 2N; \quad k, m=1, 2,..., 2N$$

where $\{\bar{\bar{Y}}^0_j\}$ and $\{\bar{\bar{Y}}_{jm}\}$ are the partial solutions at the terminal end. The product of

$[\bar{\bar{c}}^{\,\bullet}_{kj}]$ and $[\bar{\bar{Y}}_{jm}]$ is a square $N \times N$ matrix and thus $\{\zeta_m\}$ may be determined by

$$\{\zeta_m\} = -\left[\left[\bar{\bar{c}}^{\,\bullet}_{kj}\right]\left[\bar{\bar{Y}}_{jl}\right]\right]^{-1}\left\{\{\bar{\bar{d}}^{\,\bullet}_m\} + \left[\bar{\bar{c}}^{\,\bullet}_{mj}\right]\{\bar{\bar{Y}}^0_j\}\right\}$$

(3.2.6)

$$j=1, 2,..., 2N; \quad k, l, m=1,2,...,N$$

With $\{\zeta_m\}$ determined, a final integration of Eq.(3.1.3) can be performed with determined initial values

$$\{\bar{Y}_j\} = \{\bar{Y}^0_i\} + \left[\bar{Y}_{ik}\right]\{\zeta_k\}$$

(3.2.7)

$$j=1, 2,..., 2N$$

$$k=1, 2,..., N$$

3.3 Suppression Method

For a linear system of order 2N, N quantities are assumed at the starting end and N boundary conditions are satisfied at the terminal end. The correct solution corresponds to some combination of initial values at the starting end that produce boundary quantities satisfying the terminal boundary conditions. Partial solutions for one particular solution and N homogeneous solutions are integrated simultaneously along the cable scope by assuming N initial values which satisfy the N boundary conditions at the starting end. The growth of extraneous erroneous solutions is controlled by selecting suppression points at locations along the scope where magnitudes of the dependent variables exceed a prescribed limit. At each suppression

point artificial boundary conditions are then satisfied and a set of coefficients required for recombination of solutions at prior points are determined. The suppression is then performed for the partial solutions at the present and all previous suppression points. The resulting suppressed partial solutions at all suppression points are stored in order to restart the integration process within the space between successive suppression points. The integration then continues until another suppression point is required. This process is repeated until the terminal point at the far end of the cable is reached where the terminal boundary conditions are satisfied. The coefficients for recombination so as to satisfy the terminal boundary conditions are then used to determine the final partial solutions at all previous suppression points. The final combined solution is obtained by performing direct integration between all the suppression points starting with final particular partial solutions at each suppression point. The detailed mathematical treatment of the suppression process for a quasi-linearized two-point boundary value problem of order 2N is outlined in the following.

Let the partial solution vectors at a suppression point be represented by $\{Y_i^k\}$, $i=1,2,...,2N$; $k=0,1,2,...,N$. Where the superscript $k=0$ represents a particular solution and $k=1,2,...,N$ represent N homogeneous solutions. Whenever some quantities in the partial solution have become large compared with the prescribed criteria, suppression is accomplished by requiring that the partial solutions satisfy a set of independent artificial boundary conditions. It should be noted that for a system of order 2N, only N boundary conditions can be satisfied at terminal or suppression points. In other words, out of 2N quantities in the partial solutions only N quantities

can be chosen to be suppressed. The choice of these N quantities is arbitrary but must

be independent.

Once the N quantities have been be chosen, the unsuppressed partial solutions

of these N quantities are represented by $\{h_j^k\}$, j=1,2,...,N; k=0,1,2,...,N. Again,

k=0 designates a particular solution and k=1,2,...,N correspond to N homogeneous

solutions. The homogeneous partial solutions of these N quantities are collected in

matrix form as

$$[H_{jl}] = \begin{bmatrix} h_{11} & \cdots & h_{1N} \\ \vdots & & \vdots \\ h_{NI} & \cdots & h_{NN} \end{bmatrix} = \left[\{h_j^1\} \ \{h_j^2\} \ \{h_j^3\} \right] \tag{3.3.1}$$

$$j,l=1,2,...,N$$

The artificial boundary values are represented by the vectors $\{p_j^k\}$ for the

particular and homogeneous partial solutions with the element p_{jk} specified.

(j=1,2,...,N; k=0,1,2,...,N).

$$\{p_j^0\} = \begin{Bmatrix} p_{10} \\ \cdot \\ \cdot \\ \cdot \\ \cdot \\ p_{N0} \end{Bmatrix}, \ \{p_j^1\} = \begin{Bmatrix} p_{11} \\ 0 \\ \cdot \\ \cdot \\ \cdot \\ 0 \end{Bmatrix}, \ \cdots \ , \ \{p_j^l\} = \begin{Bmatrix} 0 \\ \cdot \\ p_{ll} \\ \cdot \\ \cdot \\ 0 \end{Bmatrix}, \ \{p_j^N\} = \begin{Bmatrix} 0 \\ \cdot \\ \cdot \\ \cdot \\ \cdot \\ p_{NN} \end{Bmatrix} \tag{3.3.2}$$

In order to suppress these N quantities, the following artificial boundary

conditions on all partial solutions, particular plus homogeneous, are required to be

satisfied at the suppression point

$$[H_{jl}]\{\zeta_l^k\} + \{h_j^k\} = \{p_j^k\} \qquad (3.3.3)$$

$$j, l=1, 2,..., N; \ k=0, 1, 2,..., N$$

where

[H_{jl}] = homogeneous partial solution matrix of the N quantities to be

suppressed,

$\{\zeta_l^k\}$ = suppression coefficients vector for the kth partial solution of the N

quantities,

$\{h_j^k\}$ = unsuppressed kth partial solution vector of the N quantities

$\{p_j^k\}$ = specified artificial boundary values vector for the kth partial solution

of the N quantities.

The vector of suppression coefficients for the kth partial solution of N

quantities can then be determined as

$$\{\zeta_l^k\} = [H_{il}]^{-1}\left(\{p_j^k\} - \{h_j^k\}\right)$$

$$(3.3.4)$$

$$j,l=1,2,...,N; \ k=0,1,2,...N$$

The suppressed partial solution vectors at the present and all previous

suppression points can then be obtained by:

$$\{\underline{Y}_i^k\} = \{Y_i^k\} + [Y_{il}]\{\zeta_l^k\} \qquad (3.3.5)$$

$$i=1, 2,..., 2N; \ k=0,1,2,...,N;$$

$$l=1,2,...,N$$

where $\{\underline{Y}_i^k\}$ and $\{Y_i^k\}$ are the suppressed and unsuppressed kth partial solution vectors

at suppression point, respectively, and $[Y_{il}]$ is the unsuppressed homogeneous partial

solution matrix of order $2N \times N$ at the subject suppression point.

Note that at the mth suppression point the suppression coefficients obtained are

used to suppress not only the solution at the mth suppression point, but also the

solutions at all the previous suppression points from initial point to the current

suppression point.

This marching process is continued until the terminal point is reached. The

terminal point is a special suppression point at which only the particular solution needs

to be suppressed to the terminal boundary conditions, with the suppression, or

combination, coefficients vector determined by the terminal boundary conditions as

in Eqs.(3.2.6). Again, one must note that the suppression coefficients vector obtained

at the terminal end should be used to suppress the particular partial solutions of all

the previous suppression points.

3.4 Application to Cable Problem

The general description of the numerical methods, including Newton-Raphson

quasi-linearization, decomposition technique of linear two-point boundary-value

problem and suppression method have been presented in the previous sections. It is

now possible to apply these methods to the dynamic simulation algorithm for the

cable/lumped-body system.

3.4.1 Quasi-linearization of the Governing Equations

In terms of estimates of the dependent variables $\dot{X}_i^*$, ϕ_j^* and T^*, the governing equations (2.5.6a) through (2.5.6c) for cable segment can be expanded in Taylor series.

$$
\frac{d}{ds_0}\begin{Bmatrix} \dot{X}_i \\ \phi_j \\ T \end{Bmatrix} = \begin{bmatrix} \dfrac{\partial f_i^*}{\partial \dot{X}_k} & \dfrac{\partial f_i^*}{\partial \phi_l} & \dfrac{\partial f_i^*}{\partial T} \\[3mm] \dfrac{\partial g_j^*}{\partial \dot{X}_k} & \dfrac{\partial g_j^*}{\partial \phi_l} & \dfrac{\partial g_j^*}{\partial T} \\[3mm] \dfrac{\partial h^*}{\partial \dot{X}_k} & \dfrac{\partial h^*}{\partial \phi_l} & \dfrac{\partial h^*}{\partial T} \end{bmatrix} \begin{Bmatrix} \dot{X}_k - \dot{X}_k^* \\ \phi_l - \phi_l^* \\ T - T^* \end{Bmatrix} + \begin{Bmatrix} f_i^* \\ g_j^* \\ h^* \end{Bmatrix} \qquad (3.4.1)
$$

$$i,k=1,2,\ldots,N$$

$$j,l \in \{1,2\ldots,N \setminus e\}$$

where

$$
f_i^* = (1+\epsilon^*)\,\eta_i^* + \sum_{n=1}^{3} n\, a_n\, (T^*)^{n-1}\, \phi_i^*\, \xi^* \qquad (3.4.2a)
$$

$$
g_j^* = \frac{1}{T^*}(\delta_{jk}-\phi_j^*\,\phi_k^*)\left(ma_k^* - F_{I0k}^* - (1+\epsilon^*)^{\frac{1}{2}} F_{D0k}^* - W_B\delta_{1k}\right) \qquad (3.4.2b)
$$

$$
h^* = \phi_k^*\left(ma_k^* - F_{I0k}^* - (1+\epsilon^*)^{\frac{1}{2}} F_{D0k}^* - W_B\delta_{1k}\right) \qquad (3.4.2c)
$$

and

$$\frac{\partial f_i^*}{\partial \dot{X}_k} = 0 \tag{3.4.2d}$$

$$\frac{\partial f_i^*}{\partial \phi_l} = \left[\frac{1+\epsilon^*}{\alpha \Delta t} + \xi^* \sum_{I=2}^{3} I (I-1) a_I (T^*)^{I-2} \right] \Delta_{il} \tag{3.4.2e}$$

$$\frac{\partial f_i^*}{\partial T} = \sum_{I=1}^{3} I a_I (T^*)^{I-1} \left[\frac{\phi^*}{\alpha \Delta t} + \eta_i^* \right] \\ + \sum_{n=2}^{3} n (n-1) a_n (T^*)^{n-2} \phi_i^* \xi^* \tag{3.4.2f}$$

$$\frac{\partial g_j^*}{\partial \dot{X}_k} = \frac{1}{T^*}(\delta_{ji}-\phi_j^* \phi_i^*) \left[\frac{m}{\alpha \Delta t}\delta_{ik} - \left[\frac{\partial F_{IOi}^*}{\partial \dot{X}_k} + (1+\epsilon^*) \frac{\partial F_{DOi}^*}{\partial \dot{X}_k} \right] \right] \tag{3.4.2g}$$

$$\frac{\partial g_j^*}{\partial \phi_l} = -\frac{1}{T^*} (\Delta_{kl}\phi_j^* + \delta_{jl}\phi_k^*) \left(ma_k^* - F_{IOk}^* - (1+\epsilon^*)^{\frac{1}{2}} F_{DOk}^* - W_B \delta_{1k} \right) \\ -\frac{1}{T^*} (\delta_{jk} - \phi_j^* \phi_k^*) \left[\frac{\partial F_{IOk}^*}{\partial \phi_l} + (1+\epsilon^*) \frac{\partial F_{DOk}^*}{\partial \phi_l} \right] \tag{3.4.2h}$$

$$\frac{\partial g_j^*}{\partial T} = \frac{1}{T^{2*}}(\delta_{jk}-\phi_j^* \phi_k^*) \left(ma_k^* - F_{IOk}^* - (1+\epsilon^*)^{\frac{1}{2}} F_{DOk}^* - W_B \delta_{1k} \right) \\ + \frac{1}{2 T^* (1+\epsilon^*)^{\frac{1}{2}}} (\delta_{jk}-\phi_j^* \phi_k^*) \sum_{n=1}^{3} n a_n (T^*)^{n-1} F_{DOk}^* \tag{3.4.2i}$$

$$\frac{\partial h^*}{\partial \dot{X}_k} = \phi_i^* \left[\frac{m}{\alpha \Delta t}\delta_{ik} - \left[\frac{\partial F_{IOi}^*}{\partial \dot{X}_k} + (1+\epsilon^*)^{\frac{1}{2}} \frac{\partial F_{DOi}^*}{\partial \dot{X}_k} \right] \right] \tag{3.4.2j}$$

$$\frac{\partial h^*}{\partial \phi_l} = \Delta_{kl} \left(ma_k^* - F_{IOk}^* - (1+\epsilon^*)^{\frac{1}{2}} F_{DOk}^* - W_B \delta_{1k} \right) \\ - \phi_k^* \left[\frac{\partial F_{IOk}^*}{\partial \phi_l} + (1+\epsilon^*)^{\frac{1}{2}} \frac{\partial F_{DOk}^*}{\partial \phi_l} \right] \tag{3.4.2k}$$

$$\frac{\partial h^*}{\partial T} = -\frac{1}{2\,(1+\epsilon^*)^{\frac{1}{2}}} \sum_{n=1}^{3} n\, a_n\, (T^*)^{n-1}\, \phi_k^*\, F_{D0k}^* \tag{3.4.21}$$

In Eqs.(2.3.2), the time derivatives of the dependent variables, a_i^*, η_i^* and ξ_i^*, may be approximated by Eqs.(2.5.1a) through (2.5.1c). The hydrodynamic inertia and drag forces, F_{I0k} and F_{D0k}, can be calculated by Eqs.(2.3.4) and (2.3.7). The derivatives of F_{I0k} and F_{D0k} with respect to the dependent variables are found to be

$$\frac{\partial F_{F0i}^*}{\partial \dot{X}_k} = \left(\delta_{ik} - \phi_i^*\, \phi_k^*\right)\left[-\frac{\alpha_4}{\alpha \Delta t}\right] \tag{3.4.2m}$$

$$\frac{\partial F_{D0i}^*}{\partial \dot{X}_k} = -\alpha_1\, q^{n*}\delta_{ik} - \alpha_1 \frac{q_i^{n*}\, q_k^{n*}}{q^{n*}} + (\alpha_1\, q^{n*} - \alpha_2\, q^{t*})\, \phi_i^*\, \phi_k^*$$
$$+ \left[\alpha_1 \frac{q_i^{n*}\, q_m^{n*}}{q^{n*}} - \alpha_2 \frac{q_i^{t*}\, q_m^{t*}}{q^{t*}}\right]\phi_m^*\, \phi_k^* \tag{3.4.2n}$$

$$\frac{\partial F_{I0i}^*}{\partial \phi_l} = -(\Delta_{il}\, \phi_k^* + \Delta_{kl}\phi_i^*)\,(\alpha_3\ddot{u}_k^* - \alpha_4 a_k^*) \tag{3.4.2o}$$

$$\frac{\partial F_{D0i}^*}{\partial \phi_l} = -q_k^*\,(\alpha_1\, q^{n*} - \alpha_2\, q^{t*})\,(\Delta_{il}\phi_k^* + \Delta_{kl}\phi_i^*)$$
$$- q_k^*\left[\alpha_1 \frac{q_i^{n*}\, q_m^{n*}}{q^{n*}} - \alpha_2 \frac{q_i^{t*}\, q_m^{t*}}{q^{t*}}\right](\Delta_{ml}\phi_k^* + \Delta_{kl}\phi_m^*) \tag{3.4.2p}$$

The constants α_1, α_2, α_3 α_4, the ith components of the relative velocity tangent and normal to the cable, q_i^t and q_i^n, respectively, and the magnitude of the relative velocities tangent and normal to the cable, q^t and q^n, respectively, can also be found in Eqs.(2.3.4) and (2.3.7)

The δ_{ij} and Δ_{ij} are defined as

$$\delta_{ij} = \begin{cases} 0 & i \neq j \\ 1 & i = j \end{cases} \tag{3.4.2q}$$

$$\Delta_{ij} = \begin{cases} 0 & i \neq j, \quad i \neq e \\ 1 & i = j \\ -\dfrac{\phi_j}{\phi_e} & i = e \end{cases} \tag{3.4.2r}$$

where ϕ_e is the eliminated direction cosine.

One should note that the potential singularity term, i.e. $1/T^*$, is only present in Eqs.(3.4.2g) through (3.2.2i).

3.4.2 Quasi-linearization of Force Boundary Conditions

Intermediate Body Boundary Conditions

The governing equations of the intermediate body are treated as internal boundary conditions. In order to deal with the discontinuities when the integration comes to the intermediate bodies, we need to express the unknown dependent variables "after" the body, $^a\phi_j$ and ^aT, in terms of the known dependent variables "before" the body, $^b\phi_j$ and ^bT using the governing equation (2.6.7).

$$\begin{Bmatrix} ^a\phi_j \\ ^aT \end{Bmatrix} = [J^*_{mn}] \begin{Bmatrix} \dot{X}_k - \dot{X}_k^* \\ ^b\phi_l - {}^b\phi_l^* \\ ^bT - {}^bT^* \end{Bmatrix} + \begin{Bmatrix} ^a\phi_j^* \\ ^aT^* \end{Bmatrix} \tag{3.4.3a}$$

$$m,k = 1,2,...N; \ j,l \in J; \ n = 1, 2,..., 2N$$

where

$$
{}^{a}T_i^{\ *} = -(M+\rho\ C_A V)a_i^{\ *} + (c_A+1)\rho V\ \ddot{u}_i^{\ *} + \beta q^{\ *} q_i^{\ *} + P_i(t) + P_{0i}
$$
$$
+ W\delta_{1i} - k(X_i-X_{0i}) - {}^{b}\phi_i^{\ *}\ {}^{b}T^{\ *}
$$
(3.4.3b)

$$
{}^{a}T^{\ *} = ({}^{a}T_i^{\ *}\ {}^{a}T_i^{\ *})^{\frac{1}{2}}
$$
(3.4.3c)

$$
{}^{a}\phi_j^{\ *} = \frac{{}^{a}T_j^{\ *}}{{}^{a}T^{\ *}}
$$
(3.4.3d)

and $[J_{mn}]$ is the Jacobian matrix of order $N \times 2N$.

$$
[J_{mn}^{\ *}] = \begin{bmatrix} \dfrac{\partial\ {}^{a}\phi_j^{\ *}}{\partial\dot{X}_k} & \dfrac{\partial\ {}^{a}\phi_j^{\ *}}{\partial\ {}^{b}\phi_l} & \dfrac{\partial\ {}^{a}\phi_j^{\ *}}{\partial\ {}^{b}T} \\[3ex] \dfrac{\partial\ {}^{a}T^{\ *}}{\partial\dot{X}_k} & \dfrac{\partial\ {}^{a}T^{\ *}}{\partial\ {}^{b}\phi_l} & \dfrac{\partial\ {}^{a}T^{\ *}}{\partial\ {}^{b}T} \end{bmatrix}
$$
(3.4.3e)

in which

$$
\frac{\partial\ {}^{a}\phi_j^{\ *}}{\partial\ {}^{b}\phi_l} = \frac{{}^{b}T^{\ *}}{{}^{a}T^{\ *}}\left({}^{b}\Delta_{jl} - {}^{a}\phi_j^{\ *}\ {}^{a}\phi_i^{\ *}\ {}^{b}\Delta_{il}\right)
$$
(3.4.3f)

$$
\frac{\partial\ {}^{a}\phi_j^{\ *}}{\partial\ {}^{b}T} = \frac{1}{{}^{a}T^{\ *}}\left({}^{b}\phi_j^{\ *} - {}^{a}\phi_j^{\ *}\ {}^{b}\phi_i^{\ *}\ {}^{a}\phi_i^{\ *}\right)
$$
(3.4.3g)

$$
\frac{\partial\ {}^{a}T^{\ *}}{\partial\dot{X}_k} = {}^{a}\phi_i^{\ *}\left[\frac{(M+\rho\ C_A V)}{\alpha\ \Delta t}\delta_{ik} + \beta\left[q^{\ *}\delta_{ik} + \frac{q_i^{\ *} q_k^{\ *}}{q^{\ *}}\right]\right]
$$
(3.4.3h)

$$
\frac{\partial\ {}^{a}T^{\ *}}{\partial\ {}^{b}\phi_l} = {}^{b}T^{\ *}\ {}^{a}\phi_i^{\ *}\ {}^{b}\Delta_{il}
$$
(3.4.3i)

$$\frac{\partial^a T^*}{\partial^b T} = {}^b\phi_i^* \, {}^a\phi_i^*$$

(3.4.3j)

with

$${}^b\Delta_{ij} = \begin{cases} 0 & i \neq j, \quad i \neq e \\ 1 & i = j \\ -\dfrac{{}^b\phi_j}{{}^b\phi_e} & i = e \end{cases}$$

(3.4.3k)

Boundary Body Boundary Conditions

Eqs.(2.6.7) may be written in quasi-linearized form as

$$I_i(\dot{X}_k, \phi_l, T) = [J_{ij}^*] \begin{Bmatrix} \dot{X}_k - \dot{X}_k^* \\ \phi_l - \phi_l^* \\ T - T^* \end{Bmatrix} + \{I_i^*\}$$

(3.4.4a)

$$i,k = 1,2,\ldots,N; \; j = 1,2,\ldots,2N;$$

$$l \in \{1,2,\ldots,n \setminus e\}$$

where

$$I_i^* = -(M + \rho C_A V)a_i^* + (C_A + 1)\rho V \ddot{u}_i^* + \beta \, q^* q_i^*$$
$$+ P_i(t) + P_{oi} + W\delta_{1i} - K(X_i - X_{0i}) \pm \phi_i^* T^*$$

(3.4.4b)

$$[J_{ij}^*] = \left[\frac{\partial I_i^*}{\partial \dot{X}_k} \quad \frac{\partial I_i^*}{\partial \phi_l} \quad \frac{\partial I_i^*}{\partial T} \right]$$

(3.4.4c)

$$\frac{\partial I_i^*}{\partial \dot{X}_k} = - \left[\frac{(M + \rho C_A V)}{\alpha \Delta t}\delta_{ik} + \beta \left[q^* \delta_{ik} + \frac{q_i^* q_k^*}{q^*} \right] \right]$$

(3.4.4d)

$$\frac{\partial I_i^*}{\partial \phi_l} = \begin{cases} T^*\Delta_{il} & \textit{if body located at } S_0 = 0 \\ -T^*\Delta_{il} & \textit{if body located at } S_0 = L_0 \end{cases}$$

(3.4.4e)

$$\frac{\partial I_i^{\bullet}}{\partial T} = \begin{cases} \phi_i^{\bullet} & \text{if body located at } S_0=0 \\ -\phi_i^{\bullet} & \text{if body located at } S_0=L_0 \end{cases} \qquad (3.4.4f)$$

Free End Boundary Conditions

The quasi-linearized form of the dynamic equilibrium equations (2.6.9) for the free end of cable may be written as

$$L_i = \begin{bmatrix} \dfrac{\partial L_i^{\bullet}}{\partial \dot{X}_k} & \dfrac{\partial L_i^{\bullet}}{\partial \phi_l} & \dfrac{\partial L_i^{\bullet}}{\partial T} \end{bmatrix} \begin{Bmatrix} \dot{X}_k - \dot{X}_k^{\bullet} \\ \phi_l - \phi_l^{\bullet} \\ T - T^{\bullet} \end{Bmatrix} + L_i^{\bullet} \qquad (3.4.5a)$$

where

$$L_i^{\bullet} = \left(-m\, a_i^{\bullet} + F_{IOi}^{\bullet} + (1+\epsilon^{\bullet})^{\frac{1}{2}} F_{DOi}^{\bullet} + W_B \delta_{1i} \right) \Delta - \phi_i^{\bullet} T^{\bullet} \qquad (3.4.5b)$$

$$\frac{\partial L_i^{\bullet}}{\partial \dot{X}_k} = \left[-\frac{m}{\alpha\, \Delta t} \delta_{ik} + \frac{\partial F_{IOi}^{\bullet}}{\partial \dot{X}_k} + (1+\epsilon^{\bullet})^{\frac{1}{2}} \frac{\partial F_{DOi}^{\bullet}}{\partial \dot{X}_k} \right] \Delta \qquad (3.4.5c)$$

$$\frac{\partial L_i^{\bullet}}{\partial \phi_l} = \left[\frac{\partial F_{IOi}^{\bullet}}{\partial \phi_l} + (1+\epsilon^{\bullet})^{\frac{1}{2}} \frac{\partial F_{DOi}^{\bullet}}{\partial \phi_l} \right] \Delta - T^{\bullet} \Delta_{il} \qquad (3.4.5d)$$

$$\frac{\partial L_i^{\bullet}}{\partial T} = \frac{\Delta}{2(1+\epsilon^{\bullet})^{\frac{1}{2}}} F_{DOi}^{\bullet} \sum_{n=1}^{3} na_n(T^{\bullet})^{n-1} - \phi_i^{\bullet} \qquad (3.4.5e)$$

In which $F_{DOi}^{\bullet}$ and $F_{IOi}^{\bullet}$ can be calculated by Eqs.(2.3.4) and (2.3.7) and $\partial F_i^{\bullet}/\partial \dot{X}_k$ and $\partial F_i^{\bullet}/\partial \phi_l$ may be found in Eqs.(3.4.2m) through (3.4.2p).

3.4.3 Application of Decomposition Technique

The quasi-linearized two-point boundary-value problem derived in the previous

section will be further decomposed into a set of initial-value problem in this section according to the solution scheme presented in Section 3.2. The following will summarize the initial-value problems and their corresponding initial partial solutions. The determination of the combination coefficients for the partial solution will also be presented accordingly.

Initial-value Problems

Equation (3.4.1) may be further decomposed into the following set of initial-value problems.

$$
\frac{d}{dS_0}
\begin{Bmatrix}
\dot{X}_i^0 \\
\phi_l^0 \\
T^0
\end{Bmatrix}
=
\begin{bmatrix}
\dfrac{\partial f_i^*}{\partial \dot{X}_k} & \dfrac{\partial f_i^*}{\partial \phi_l} & \dfrac{\partial f_i^*}{\partial T} \\[2ex]
\dfrac{\partial g_j^*}{\partial \dot{X}_k} & \dfrac{\partial g_j^*}{\partial \phi_l} & \dfrac{\partial g_j^*}{\partial T} \\[2ex]
\dfrac{\partial h^*}{\partial \dot{X}_k} & \dfrac{\partial h^*}{\partial \phi_l} & \dfrac{\partial h^*}{\partial T}
\end{bmatrix}
\begin{Bmatrix}
\dot{X}_k^0 - \dot{X}_k^* \\
\phi_l^0 - \phi_l^* \\
T^0 - T^*
\end{Bmatrix}
+
\begin{Bmatrix}
f_i^* \\
g_j^* \\
h^*
\end{Bmatrix}
\tag{3.4.6a}
$$

and

$$
\frac{d}{dS_0}
\begin{Bmatrix}
\dot{X}_{ik} \\
\phi_{jk} \\
T_k
\end{Bmatrix}
=
\begin{bmatrix}
\dfrac{\partial f_i^*}{\partial \dot{X}_k} & \dfrac{\partial f_i^*}{\partial \phi_l} & \dfrac{\partial f_i^*}{\partial T} \\[2ex]
\dfrac{\partial g_j^*}{\partial \dot{X}_k} & \dfrac{\partial g_j^*}{\partial \phi_l} & \dfrac{\partial g_j^*}{\partial T} \\[2ex]
\dfrac{\partial h^*}{\partial \dot{X}_k} & \dfrac{\partial h^*}{\partial \phi_l} & \dfrac{\partial h^*}{\partial T}
\end{bmatrix}
\begin{Bmatrix}
\dot{X}_{ik} \\
\phi_{jk} \\
T_k
\end{Bmatrix}
\tag{3.4.6b}
$$

$$
i,k = 1, 2, \ldots, N; \; j,l = \{1,2,\ldots,N \setminus e\}
$$

where

$$\{Y_i^0\} = \begin{Bmatrix} \dot{X}_i^0 \\ \phi_l^0 \\ T^0 \end{Bmatrix} \quad , \qquad [Y_{ik}] = \begin{Bmatrix} \dot{X}_{ik} \\ \phi_{jk} \\ T_k \end{Bmatrix} \tag{2.4.7}$$

are the particular solution and homogeneous solutions, respectively. For convenience, the particular and homogenous partial solutions for direction cosines and tension may be written hereafter as

$$\{\Phi_i^0\} = \begin{Bmatrix} \phi_l^0 \\ T^0 \end{Bmatrix} \quad , \qquad [\Phi_{ik}] = \begin{Bmatrix} \phi_{jk} \\ T_k \end{Bmatrix} \tag{2.4.8}$$

Initial Partial Solutions

The following initial partial solutions which satisfy the boundary conditions at a starting point are specified to initiate the numerical integration of the initial-cable problem posed by Eqs.(3.4.6).

1) Kinematic Boundary Conditions:

$$\{\bar{\dot{X}}_i^0\} = \{\bar{\dot{X}}_i^s\} \tag{3.4.9a}$$

$$[\bar{\dot{X}}_{ik}] = [0] \tag{3.4.9b}$$

$$\{\bar{\Phi}_i^0\} = \{\bar{\Phi}_i^*\} \tag{3.4.9c}$$

$$[\bar{\Phi}_{ik}] = \begin{bmatrix} 0.01 & 0 & 0 \\ 0 & 0.01 & 0 \\ 0 & 0 & \bar{T}^* \end{bmatrix} \qquad (3.4.9d)$$

$$i, k=1, 1,..., N; \; j \in \{1,2,...,N \setminus e\}$$

where $\{\bar{\dot{X}}_i^s\}$ is the known velocity vector at the starting end. If $\{\bar{\dot{X}}_i^s\} \equiv 0$, Eqs.(4.3.9)

specify a hinged (stationary) boundary condition as a special case of the kinematic

boundary conditions.

2) Force Boundary Conditions:

$$\{\bar{X}_i^0\} = \{0\} \qquad (3.4.10a)$$

$$[\bar{\dot{X}}_{ik}] = [\,I\,] \qquad (3.4.10b)$$

$$\{\bar{\Phi}_i^0\} = \{\bar{\Phi}_i^*\} + [C_{ij}^*] \left\{ \frac{\partial I_j^*}{\partial \dot{X}_k} \bar{\dot{X}}_k^* - I_j^* \right\} \qquad (3.4.10c)$$

$$[\bar{\Phi}_{ik}] = -[C_{ij}^*] \left[\frac{\partial I_j^*}{\partial \dot{X}_k} \right] \qquad (3.4.10d)$$

where [I] is an identity matrix; I_j^* and $\partial I_j^*/\partial \dot{X}_k$ can be found in Eqs.(3.4.4b) and

(3.4.4d),respectively. $[C_{ij}^*]$ is an $N \times N$ matrix written in the form

$$[C_{ij}^*] = \left[\frac{\partial I_j^*}{\partial \phi_l} \frac{\partial I_j^*}{\partial T} \right]^{-1} \qquad (3.4.10e)$$

$$[C_{ij}^{\bullet}] = \begin{bmatrix} C_1 & C_3 & C_1 \\ C_1+C_3 & 0 & C_2 \\ 0 & C_1+C_2 & C_3 \end{bmatrix} \quad if \ \phi_e = \phi_1 \tag{3.4.10f}$$

$$[C_{ij}^{\bullet}] = \begin{bmatrix} C_1+C_3 & 0 & C_1 \\ C_1 & C_3 & C_2 \\ 0 & C_1+C_2 & C_3 \end{bmatrix} \quad if \ \phi_e = \phi_2 \tag{3.4.10g}$$

$$[C_{ij}^{\bullet}] = \begin{bmatrix} C_2+C_3 & 0 & C_1 \\ 0 & C_1+C_3 & C_2 \\ C_1 & C_2 & C_3 \end{bmatrix} \quad if \ \phi_e = \phi_3 \tag{3.4.10h}$$

In Eqs.(3.4.10f) through (3.4.10h) $C_1 = \phi_1^{\bullet}\phi_1^{\bullet}$, $C_2 = \phi_2^{\bullet}\phi_2^{\bullet}$ and $C_3 = \phi_3^{\bullet}\phi_3^{\bullet}$.

For a two-dimensional problem

$$[C_{ij}^{\bullet}] = \begin{bmatrix} C_2 & C_1 \\ C_1 & C_2 \end{bmatrix} \tag{3.4.10i}$$

Intermediate Partial Solutions

In order to continue the numerical integration across an intermediate body, the partial solutions have to be updated according to the following continuity and equilibrium relations.

$$\{^a\dot{X}_i^0\} = \{^b\dot{X}_i^0\} \tag{3.4.11a}$$

$$[^a\dot{X}_{ik}] = [^b\dot{X}_{ik}] \tag{3.4.11b}$$

$$\{^a\Phi_i^0\} = \{^a\Phi_i^{\bullet}\} + [J_{ij}^{\bullet}] \begin{Bmatrix} \dot{X}_i^0 - \dot{X}_i^{\bullet} \\ {}^b\Phi_i^0 - {}^b\Phi_i^{\bullet} \end{Bmatrix} \tag{3.4.11c}$$

$$[^a\Phi_{ik}] = [J_{ij}^*] \begin{Bmatrix} [^b\dot{X}_{ik}] \\ [^b\Phi_{ik}] \end{Bmatrix} \qquad (3.4.11d)$$

$$k = 1, ..., N$$

$$j = 1, 2, ..., 2N$$

where left superscripts, "b" and "a", respectively, represent the partial solutions "before" and "after" the intermediate body if one follows the direction of spatial integration. The Jacobian matrix $[J_{ij}^*]$ can be found in Eqs.(3.4.3)

Determination of Linear Combination Coefficients

Let Eq.(3.2.6) be written in a simplified form as $[A_{ik}]\{\zeta_k\} = \{B_i\}$, the coefficients of $[A_{ik}]$ and $\{B_i\}$ may be determined as follows according to the boundary conditions at the terminal end. Then, $\{\zeta_k\}$ can be readily determined.

1) Kinematic Boundary Conditions:

$$\qquad (3.4.12a)$$

$$[A_{ik}] = [\bar{\bar{X}}_{ik}]$$

$$\{B_i\} = \{\bar{\bar{X}}_i^s - \bar{\bar{X}}_i^0\} \qquad (3.4.12b)$$

where $\{\bar{\bar{X}}_i^s\}$ is the specified velocity vector at the terminal end. If $\{\bar{\bar{X}}_i^s\} \equiv 0$, Eqs.(3.4.12) determines the combination coefficients $\{\zeta_k\}$ for the hinged (stationary) boundary condition, as a special case of the kinematic boundary condition.

2) Force Boundary Conditions

At the terminal end, the linearized force boundary conditions Eq.(3.4.4a) may be written as

$$\bar{\bar{I}}_i(\bar{\bar{X}}_k, \bar{\bar{\Phi}}_l) = [\bar{\bar{J}}_{ij}^*] \begin{Bmatrix} \bar{\bar{X}}_k - \bar{\bar{X}}_k^* \\ \bar{\bar{\Phi}}_l - \bar{\bar{\Phi}}_l^* \end{Bmatrix} + \bar{\bar{I}}_i^* = 0 \tag{3.4.13}$$

Upon substitution of Eq.(3.2.1) into (3.4.13),

$$[\bar{\bar{J}}_{ij}^*] \begin{Bmatrix} \bar{\bar{X}}_l^0 + [\bar{\bar{X}}_{lk}]\{\zeta_k\} - \bar{\bar{X}}_l^* \\ \bar{\bar{\Phi}}_l^0 + [\bar{\bar{\Phi}}_{lk}]\{\zeta_k\} - \bar{\bar{\Phi}}_l^* \end{Bmatrix} + \bar{\bar{I}}_i^* = 0$$

or

$$[\bar{\bar{J}}_{ij}^*] \begin{Bmatrix} [\bar{\bar{X}}_{lk}] \\ [\bar{\bar{\Phi}}_{lk}] \end{Bmatrix} \{\zeta_k\} = [\bar{\bar{J}}_{ij}^*] \begin{Bmatrix} \bar{\bar{X}}_l^* - \bar{\bar{X}}_l^0 \\ \bar{\bar{\Phi}}_l^* - \bar{\bar{\Phi}}_l^0 \end{Bmatrix} - \bar{\bar{I}}_i^*$$

Therefore

$$[A_{ik}] = [\bar{\bar{J}}_{ij}^*] \begin{Bmatrix} [\bar{\bar{X}}_{lk}] \\ [\bar{\bar{\Phi}}_{lk}] \end{Bmatrix} \tag{3.4.14a}$$

$$\{B_i\} = [\bar{\bar{J}}_{ij}^*] \begin{Bmatrix} \bar{\bar{X}}_l^* - \bar{\bar{X}}_l^0 \\ \bar{\bar{\Phi}}_l^* - \bar{\bar{\Phi}}_l^0 \end{Bmatrix} - \bar{\bar{I}}_i^* \tag{3.4.14b}$$

$$i, k, l = 1, 1, \ldots, N; \quad j = 1, 2, \ldots, 2N$$

where $[\bar{\bar{J}}_{ij}^*]$ and $\bar{\bar{I}}_i^*$ may be found in Eqs. (3.4.4).

For the free end boundary conditions, the equivalent expression can be derived

by replacing $\bar{l}_i^*$ and $[\bar{J}_{ij}^*]$ in Eqs.(3.4.14) by L_i^* and the corresponding Jacobian

matrix specified by Eqs.(3.4.5).

3.4.4 Application of Suppression Scheme

A general description of the suppression method has been given in Section 3.3.

In the following, the implementation of the suppression scheme is summarized.

1) Out of the 2N dependent variables, only N can be chosen to be suppressed.

   The choice of these N dependent variables is arbitrary. In the present study,

   the direction cosines and tension magnitude are selected.

2) The artificial boundary values in Eq.(3.3.5) are given as: $p_{i0}=\Phi_i^*$; $p_{ii}=0.01$,

   $(i=1,2,...N-1)$ and $p_{NN}=T^*$.

3) Whenever a direction cosine in a vector of the partial solution exceed 0.9,

   the suppression is performed on that vector for the present and all previous

   suppression points.

3.4.5 Solution Algorithms

The algorithms implementated in the computer code KBL92 is given below:

1) Input the required data and nondimensionlize all the variables.

2) Input initial configuration $\{X_i\}$, direction cosines and tension $\{\Phi_i\}$. Input or

   generate initial velocity components $\{\dot{X}_i\}$ and acceleration $\{\ddot{X}_i\}$, For restart

or time decremental problem, input cable strain $\{\epsilon\}$ and time derivative of direction cosines and tension, $\{\partial\phi_i/\partial t\}$ and $\{\partial T/\partial t\}$.

3) Initialize the payout flag and cable/bottom contact flag. IPAYOT=0, and ISTATE=0.

4) Proceed one time step $t=t^p+\Delta t$.

5) Check payout state. If time is greater than or equal to the start time of payout and the payout rate is greater than zero, IPAYOT=1.

6) Initialize the guessed solutions $\{X_i^*\}, \{\dot{X}_i^*\}$ and $\{\Phi_i^*\}$, and the previous solution $\{X_i^p\}, \{\dot{X}_i^p\}$ and $\{\Phi_i^p\}$ for all integration points. If IPAYOT=1, extrapolate the guessed and previous solutions for the new points being paid-out.

7) Generate initial partial solutions at the starting end according to Eqs.(3.4.9) or (3.4.10).

8) Integrate quasi-linearized Eqs.(3.4.6) with the initial partial solutions specified in step 7) along the cable scope using Runge-Kutta-Gill method. If necessary, suppression may be accomplished. The suppressed partial solutions at all suppression points are stored for obtaining combined solution.

9) Calculate $[A_{ik}]$ and $\{B_i\}$ by Eqs.(3.4.12) or (3.4.14) and solve for combination coefficients vector $\{\zeta_k\}$. The particular partial solutions at all previous suppression points are then suppressed using the coefficients $\{\zeta_k\}$ in order to satisfy the terminal boundary conditions.

10) Integrate the particular partial solutions between all suppression points to obtain a new solution for $\{\dot{X}_i\}$ and $\{\Phi_i\}$.

11) Update the guessed solutions with the present solutions $\{\dot{X}_i\}$ and $\{\Phi_i\}$ for the next iteration.

12) Compute coordinates $\{X_i\}$ by numerical integration of Eq.(2.4.2).

13) If X_1 coordinate of the terminal end is greater than water depth, cable/bottom contact occurs, ISTATE=1.

14) Check the convergence criteria by Eq.(3.1.6). Repeat steps 6) through 13) until the stipulated convergence criteria is met.

15) If in cable/bottom contact state, change the integration scope of the last cable segment in order to meet the constraint (2.5.11) on water depth. Repeat 6) through 15) until the constraint is met.

16) Evaluate time derivative of $\{\dot{X}_i\}$ and $\{\Phi_i\}$ by the Newmark-like implicit integration formulas (2.6.1).

17) Terminate the process if the solution has reached the steady state.

18) Print at selected time step the convergent solutions of $\{X_i\}$, $\{\dot{X}_i\}$ and $\{\Phi_i\}$.

19) Repeat steps 4) through 18) until the prescribed number of integration time steps are finished.

4.0 SAMPLE PROBLEMS

In this chapter sample problems to validate and demonstrate the capabilities of the solution algorithms developed in the previous chapters are presented. There are five sample problems.

Problem 1 investigates a pendulum oscillating in air and in water. It is selected to validate the solution algorithm by comparing the numerical and analytical solutions. This problem examines the effects of hydrodynamic damping and of numerical damping introduced by the integration scheme. A decremental results is also presented.

Problem 2 considers the dynamic response of a moored surface buoy subject to regular and irregular waves. High quality experimental data is available for comparisons from experiments recently conducted by the U.S. Naval Academy Hydromechanics Laboratory under the sponsorship of the Naval Civil Engineering Laboratory.

Problem 3 shows the transient response of a towed cable/object. The results of a similar case with three cable segments, each having different properties, is also given to demonstrate the program capability of dealing with material discontinuities.

Problem 4 is a towed cable with a free end. In order to avoid the singularity, i.e. $T=0$, at the free end of the cable, the special boundary condition developed in Section 2.5.2 is applied.

Problem 5 consists of three cable segments and two intermediate bodies being paid-out from a moving vessel and deposited onto the ocean floor. This example demonstrates the ability of the present solution algorithm to deal with payout boundary

conditions and slack-cable/ocean-bottom contact boundary conditions.

4.1 Problem 1: Pendulum Oscillating Air and in Water.

A definition sketch of the pendulum problem is shown in Fig.4.1. This example is intended to show the validity of the present solution algorithm by comparing the numerical solution to the analytical solution and to examine the numerical damping effect that may be introduced by an inappropriate integration scheme. To accomplish this, a displaced initial configuration with small initial angle (Θ_0=5.732 degree) is obtained by applying a horizontal force of 98.1 N at the body. The body is then released at time t=0 and allowed to oscillate.

The cable and body properties are summarized in the following:

Gravitational constant	= 9.81 m/s^2
Mass density of water	= 1020.0 kg/m^3

Cable:

Unstretched length	= 5.0 m
Diameter	= 0.01 m
Mass per unit length	= 0.00001 kg/m
Material	= inextensible
Normal Drag coefficient	= 1.2
Tangential drag coefficient	= 0.02
Added mass coefficient	= 1.0

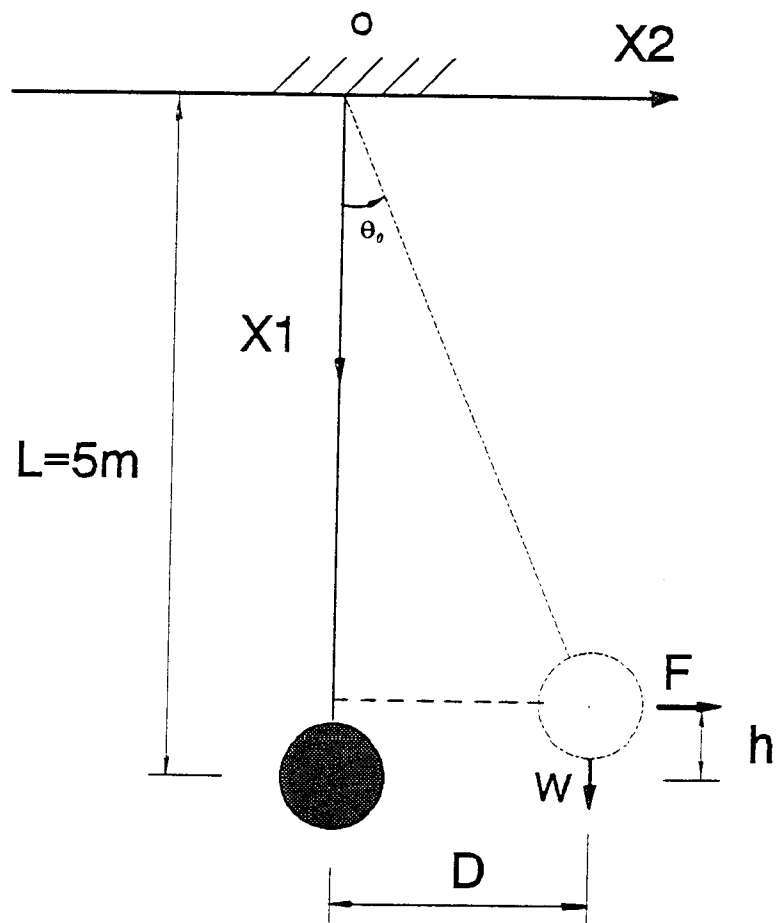Figure 4.1 Pendulum Oscillating in Air and in Water

Spherical body:

Radius   = 0.2 m

Mass   = 103.48 kg

Drag coefficient   = 1.0

Added mass coefficient   = 0.5

For the undamped (in air) small amplitude free oscillation, the analytical solution

is readily available for comparison.

Oscillation period:

$$T = 2\pi \sqrt{\frac{L}{g}} = 4.4875 \quad seconds$$

Maximum velocity at lowest point:

$$\dot{X}_{max} = \sqrt{2gh} = 0.70036 \quad m/s$$

Numerical simulation of the time history of the motion and of the velocity in the

X_2 direction are plotted in Figs.4.2 and 4.3, respectively. Numerical damping effects

(amplitude decay and period elongation) are observed for the case of $\alpha=1.0$ which

corresponds to the backward difference formula adopted in KBLDYN. On the other

hand, almost no amplitude decay (numerical damping) can be observed for the case of

$\alpha=0.5$, corresponding to the Newmark-like (Eq.(2.6.1)) implicit integration scheme. The

numerically undamped solutions ($\alpha=0.5$) for the period and the maximum velocity of the

body are 4.5 seconds and 0.7 m/s, respectively, which are in close agreement (99.7%, 100.1%) with those of the theoretical solution.

Incremental solutions for horizontal and vertical coordinates of the body in water damped oscillation are plotted along with the decremental solutions in Fig.4.4. The decremented results were obtained by using the "final" state solution, achieved by an incremental run, as the "initial" condition and integrating backward by setting a negative time step and "initial" time > 0. This so called "Time Decrement Method" was shown to be analytically sound and easy to implement and may have advantages over the "Time Increment Method" when incorporating the dynamic simulation program into an optimization and control program for designing and monitoring installation procedures of the cable/lumped-body system (Leonard,1989). It can be seen that the decremented solution reproduces the incremented solution very well over the majority of the time history. A small deviation can be detected only near the beginning of the time history. However, it was found that the decremental scheme is more sensitive than the incremental method regarding its numerical stability. When trying to obtain decremental solutions for some other examples, divergence may happens during the numerical integration.
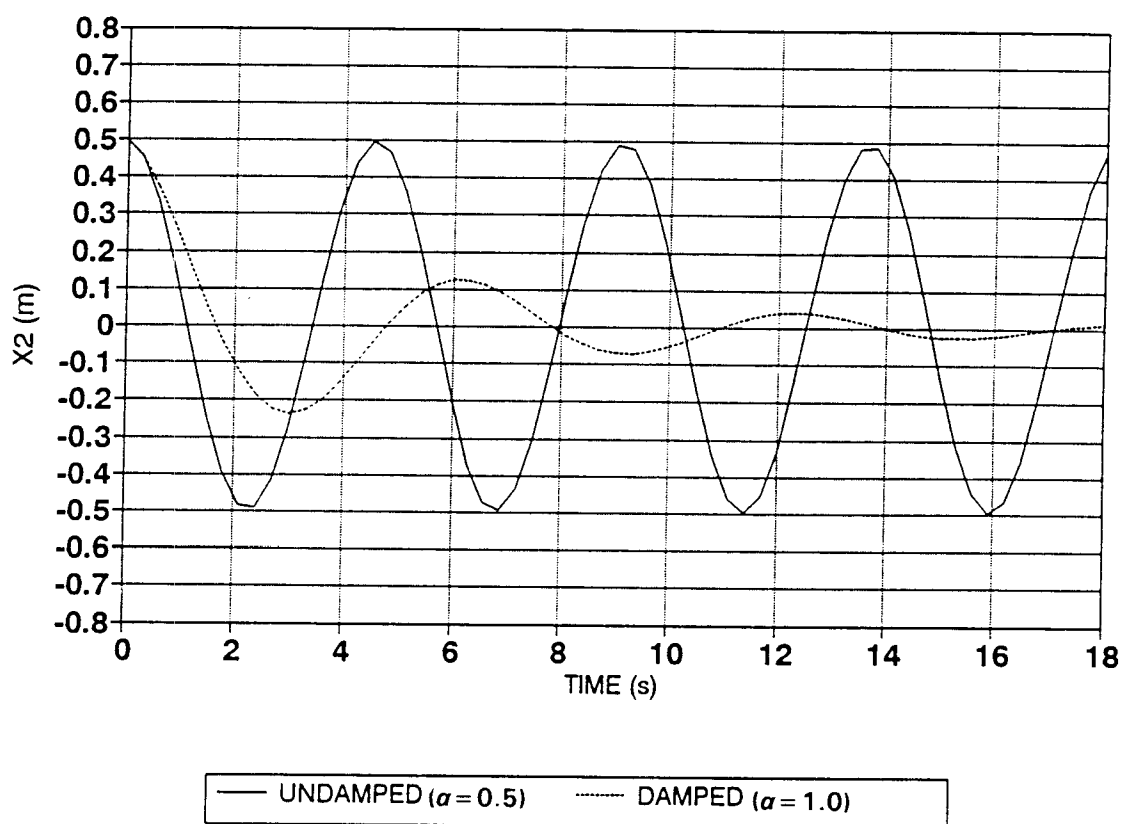
Figure 4.2 Time History of Motion of Pendulum Oscillating in Air
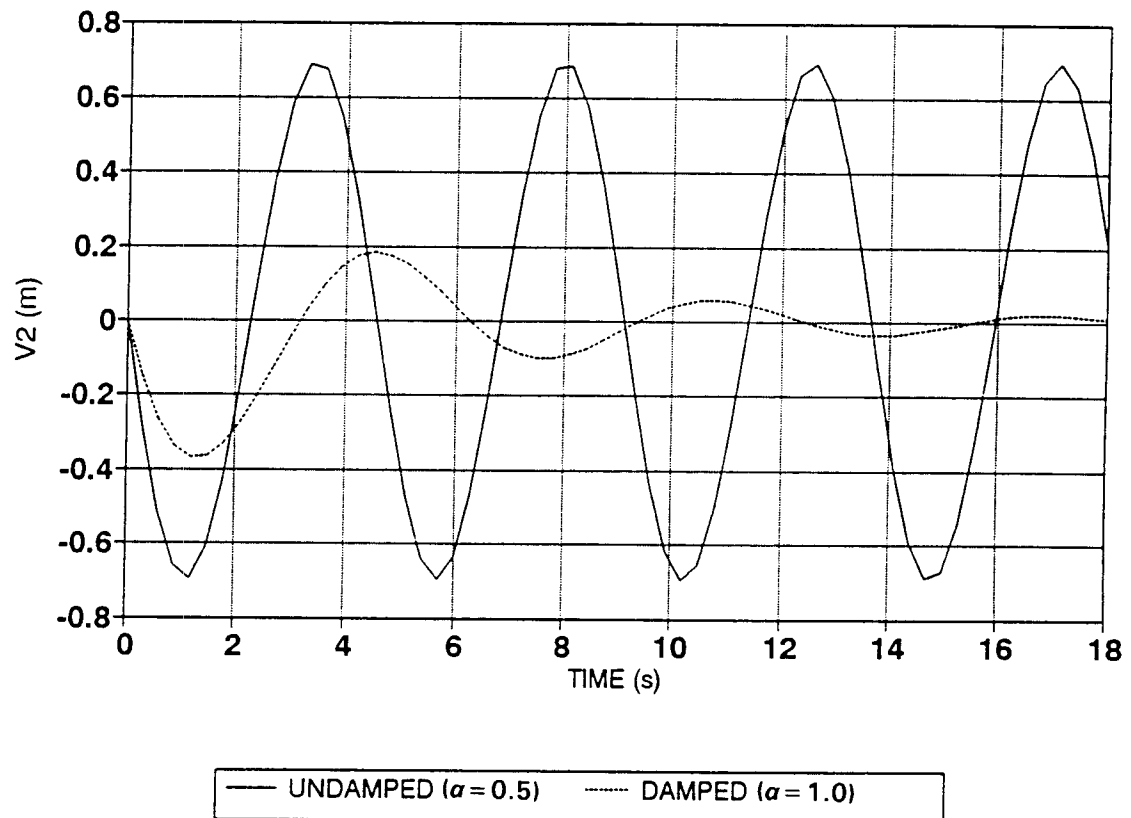
(Numerical Damping Effect)

Figure 4.3 Time History of Velocity of Pendulum Oscillating in Air
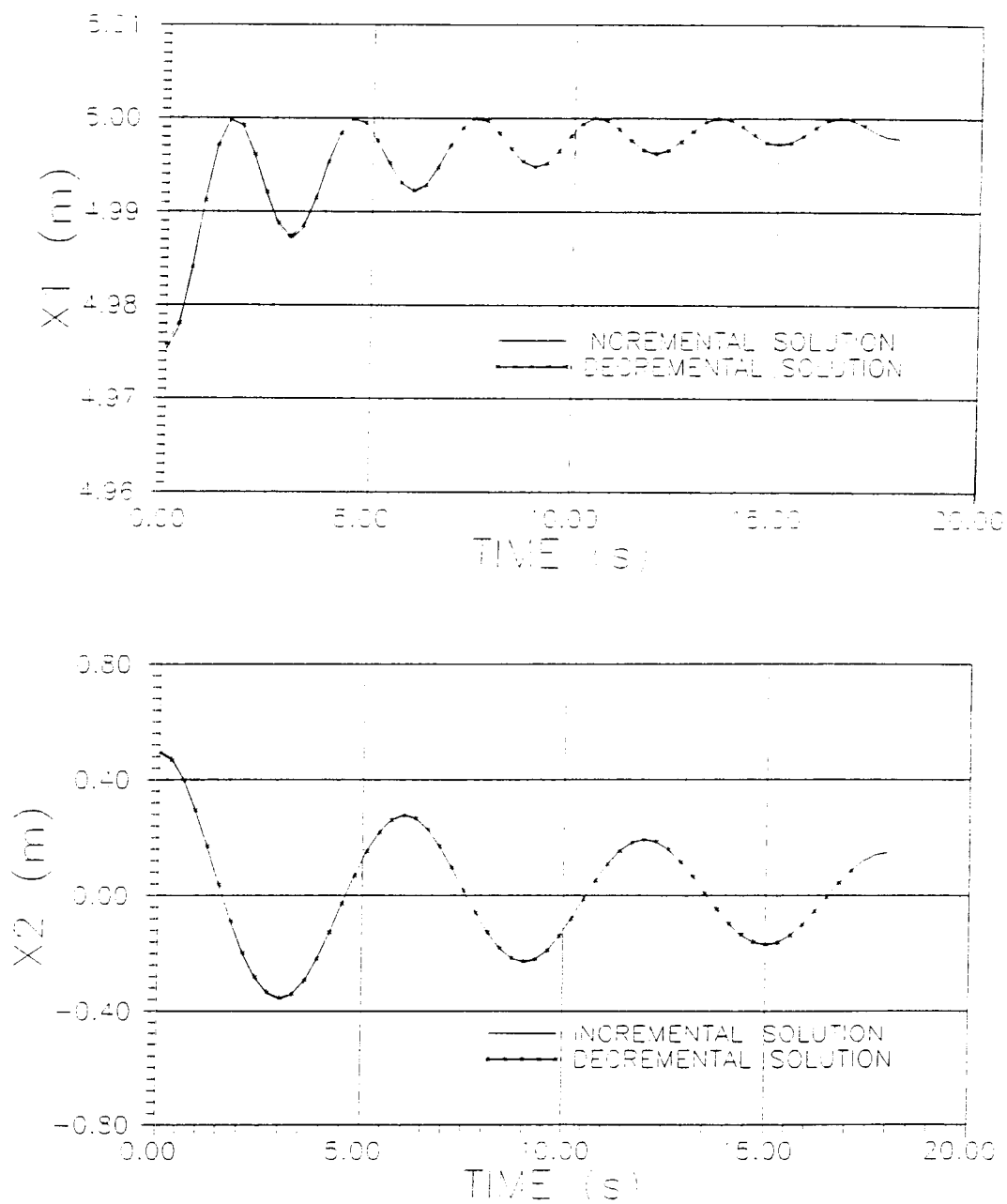
(Numerical Damping Effect)

Figure 4.4 Time History of Motion of Pendulum Oscillating in Water

(Decremented vs. Incremented Solution)

4.2 Problem 2: Wave Loads on Moored Buoy

The Naval Civil Engineering Laboratory (NCEL) and the United States Naval Academy (USNA) conducted scale model buoy tests at the USNA. Hydromechanics Laboratory in September 1989. Those tests were designed to provide experimental data for validating cable/buoy computer programs. Tethered buoys were tested in both regular and random tow-dimensional seas. Buoy responses (pitch,heave,and surge) were measured using advanced high speed video/computer system techniques. The data collected are high quality and suitable for the purpose of validating numerical simulation models of cable/buoy systems (Harris and Shields,1990)

A definition sketch is shown in Fig. 4.5 for a spherical buoy. Details of the experimental setup are given by Harris and Shields (1990). A 4-inch diameter spherical buoy floating on the water surface was moored with 17.33 feet of slack line in 16 feet deep water. Prior to data collection, waves were produced and the buoy was allowed to move to an offset position. The buoy response motions (heave, surge, pitch) and tensions at top and bottom of the mooring line were then recorded. The mooring line and buoy parameters are summarized as follows:

Gravitational constant	$= 32.2 \text{ ft/s}^2$
Mass density of water	$= 1.99 \text{ slugs/ft}^3$

Cable:

Unstretched length	$= 17.33$ ft.
Diameter	$= 0.013$ ft.
Mass per unit length	$= 0.0004503$ slugs/ft.
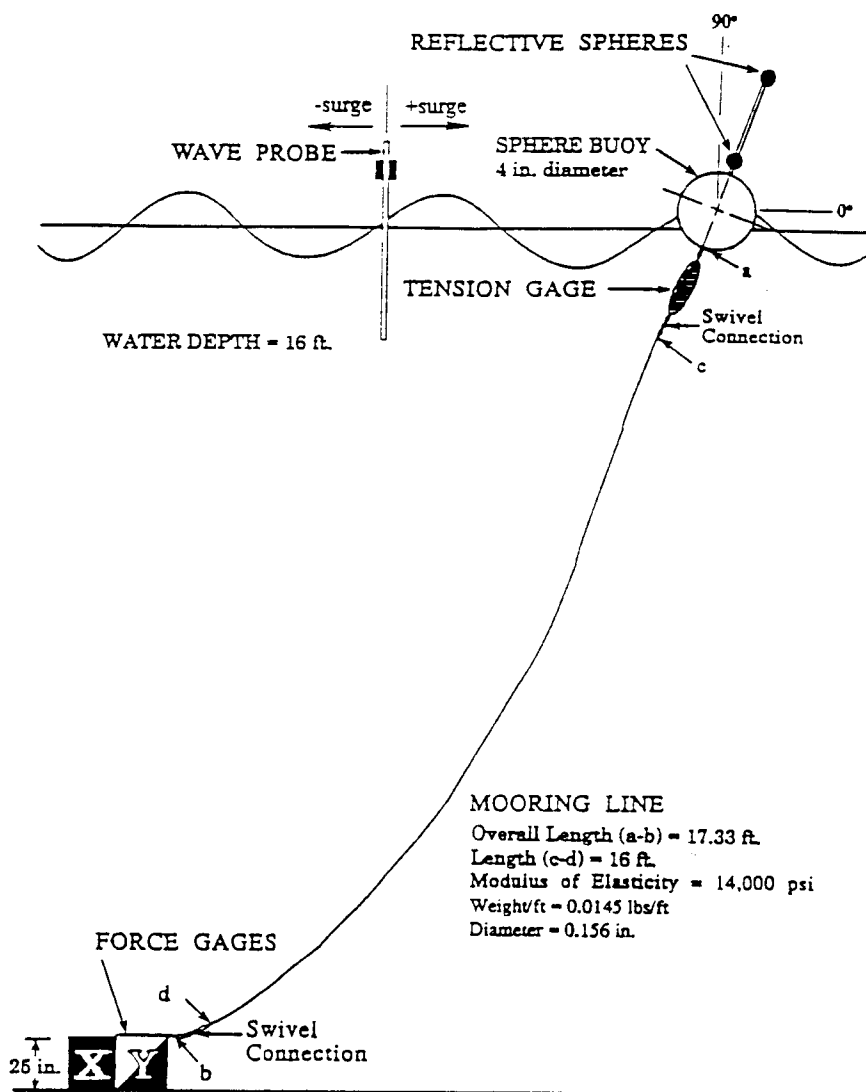
Figure 4.5 Definition Sketch of Naval Academy Experiment

Buoyant weight per unit length	= 0.006 lb/ft.
Modulus of elasticity	= 14,000 psi.
Normal Drag coefficient	= 1.2
Tangential drag coefficient	= 0.03
Added mass coefficient	= 1.0

Buoy:

Radius	= 0.16667 ft.
Mass	= 0.0158385 slugs
Drag coefficient	= 0.5
Added mass coefficient	= 0.5

To numerically simulate the experiment, the surface buoy was first statically displaced to an initial offset equilibrium position by applying a horizontal force at the buoy. The dynamic analysis of the mooring system was then conducted. The fictitious horizontal force was gradually removed so as to reproduce the real experimental condition.

Two typical test cases were chosen to make comparisons between numerical predictions and experimental measurements.

Sphere Regular Wave Test SRH30A: (wave height=1.333 ft, wave period=3.333 seconds)

The numerical integration along the cable was conducted in 61 spatial steps from the anchor to the buoy. The run was made for a total of 600 time steps with time step size of 0.4 second which is approximately 1/9 of the period of incident waves. A

nondimensional error tolerance of 0.05 was selected for the convergence criteria in the iteration process. The Newton-Raphson process typically converged in about 2 to 4 iterations.

As shown in Figs.4.6 and 4.7, the time histories of buoy heave and surge obtained by the present numerical model compare favorably with the experimental measurements. However, the present simulation seems to underestimate the buoy heave motion by 10 percent and the surge by 16 percent. This may be attributed to the buoy-water-air interaction and the buoy rotation effects. The tension history at the top of the mooring line and at the anchor are given in Fig.4.8. Unfortunately, the measured tension history can not be used for comparison because the tension was not accurately recorded in the experiment due to sensitivity problems associated with the tension gage.

Sphere Irregular Wave Test SIH30B: (Bretschneider spectrum: significant wave height=1.333 ft., peak frequency=0.3 second.)

The predicted random response of buoy heave and surge are shown in Fig.4.9 and Fig.4.10. In order to compare them with the experimental records, it is convenient to chose a coordinate system such that the mean value for each time history of the response is zero. The Root Mean Square value (RMS) for the numerical results and experimental records were then calculated by

$$RMS = \sqrt{\frac{1}{T_d} \int_0^{T_d} h^2(t) \ dt}$$

where h(t) is time history of the response, T_d is the duration of the time history.

The RMS values for the buoy heave and surge motions of both numerical prediction and experimental records are compared in Table 4.1.

Table 4.1 Comparison of RMS Values of Buoy Random

Heave and Surge Motions (unit: inch)

	Numerical results	Experimental data
Heave	3.3415	3.9028
Surge	3.1582	5.3256

The comparison of the RMS values between predicted and measured random heave response gives acceptable 14 percent relative error. However, for random surge response the relative error of RMS value is as large as 40.7 percent. Again, this may have resulted from the buoy-water-air interaction and buoy rotational effects. The random response of the tension at the top of the mooring line is given in Fig.4.11. Again, the experimental data collected could not be used reliably for comparison.
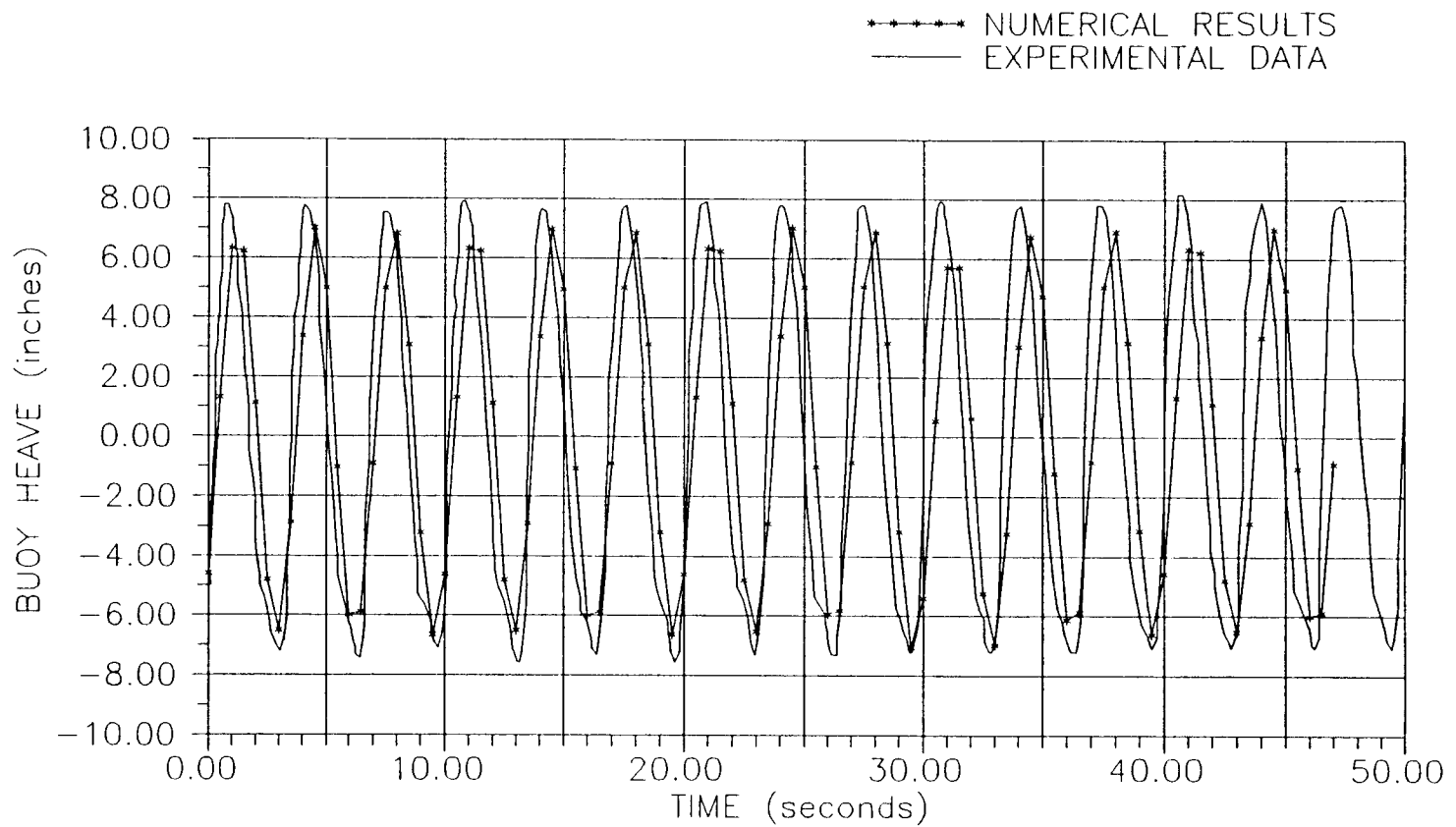
Figure 4.6 Time History of Buoy Heave
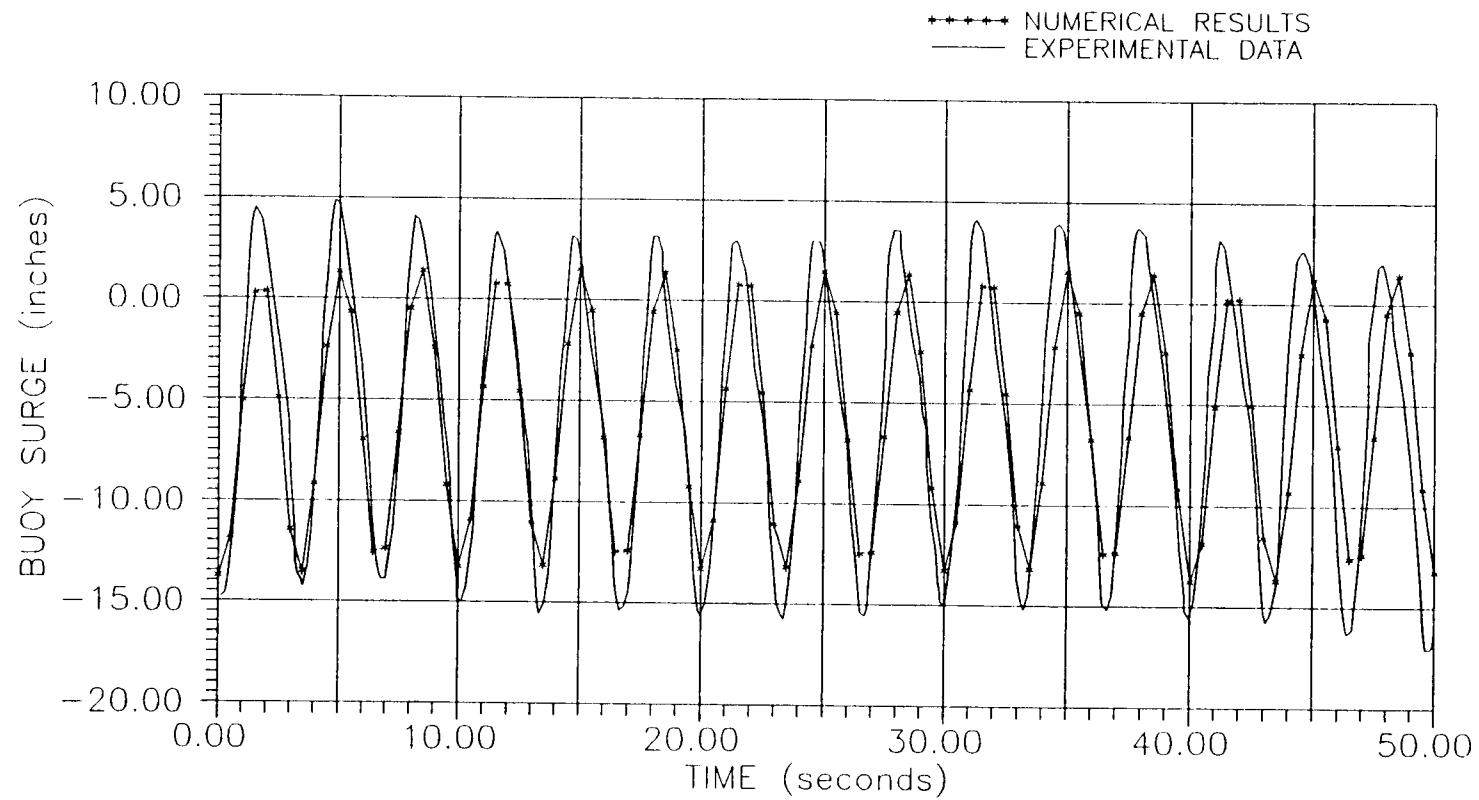
(Numerical vs. Experimental Solution)

Figure 4.7 Time History of Buoy Surge

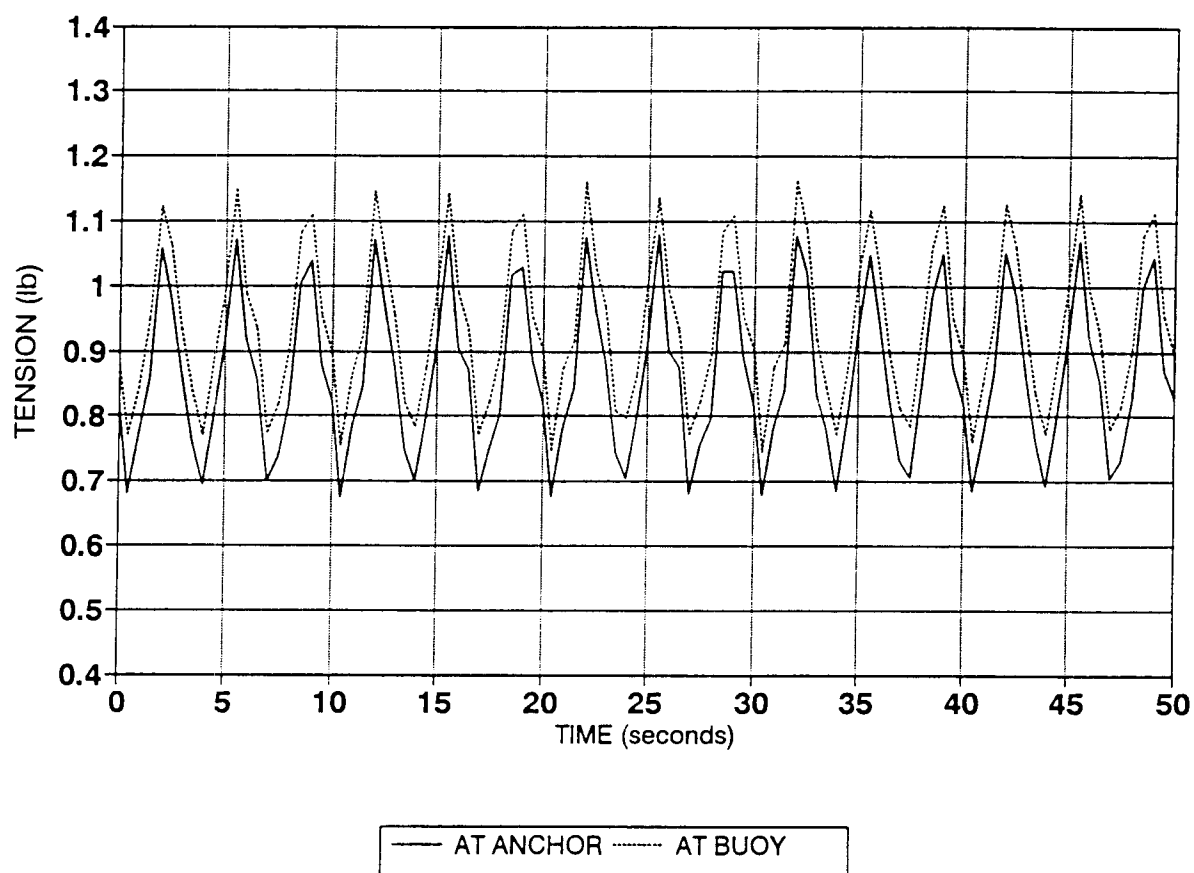(Numerical vs. Experimental Solution)

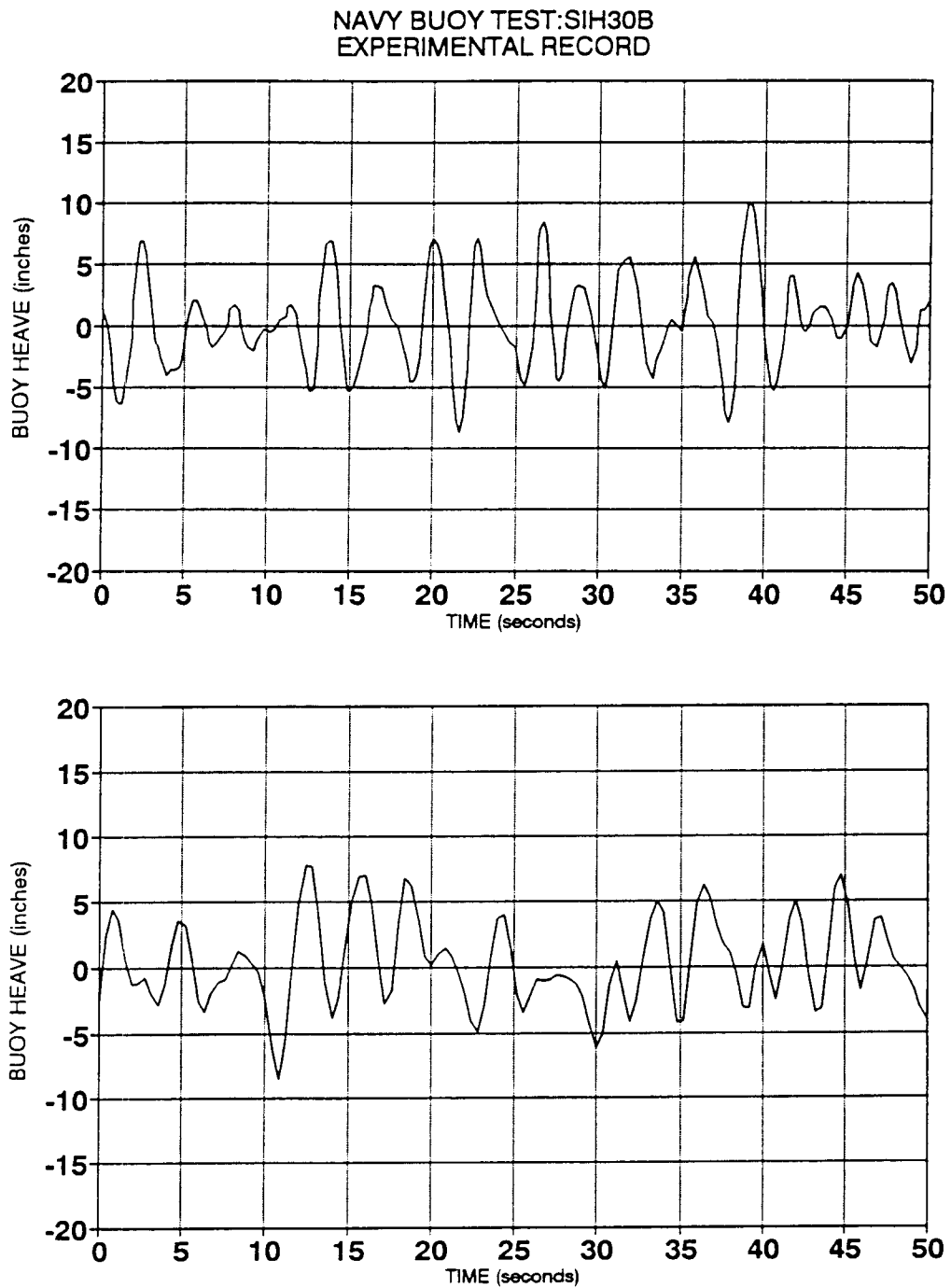Figure 4.8 Predicted Time History of Tension at Surface Buoy

and at the Anchor

NAVY BUOY TEST:SIH30B
EXPERIMENTAL RECORD

Figure 4.9 Random Response of Surface Buoy Heave

(Numerical vs. Experimental Solution)
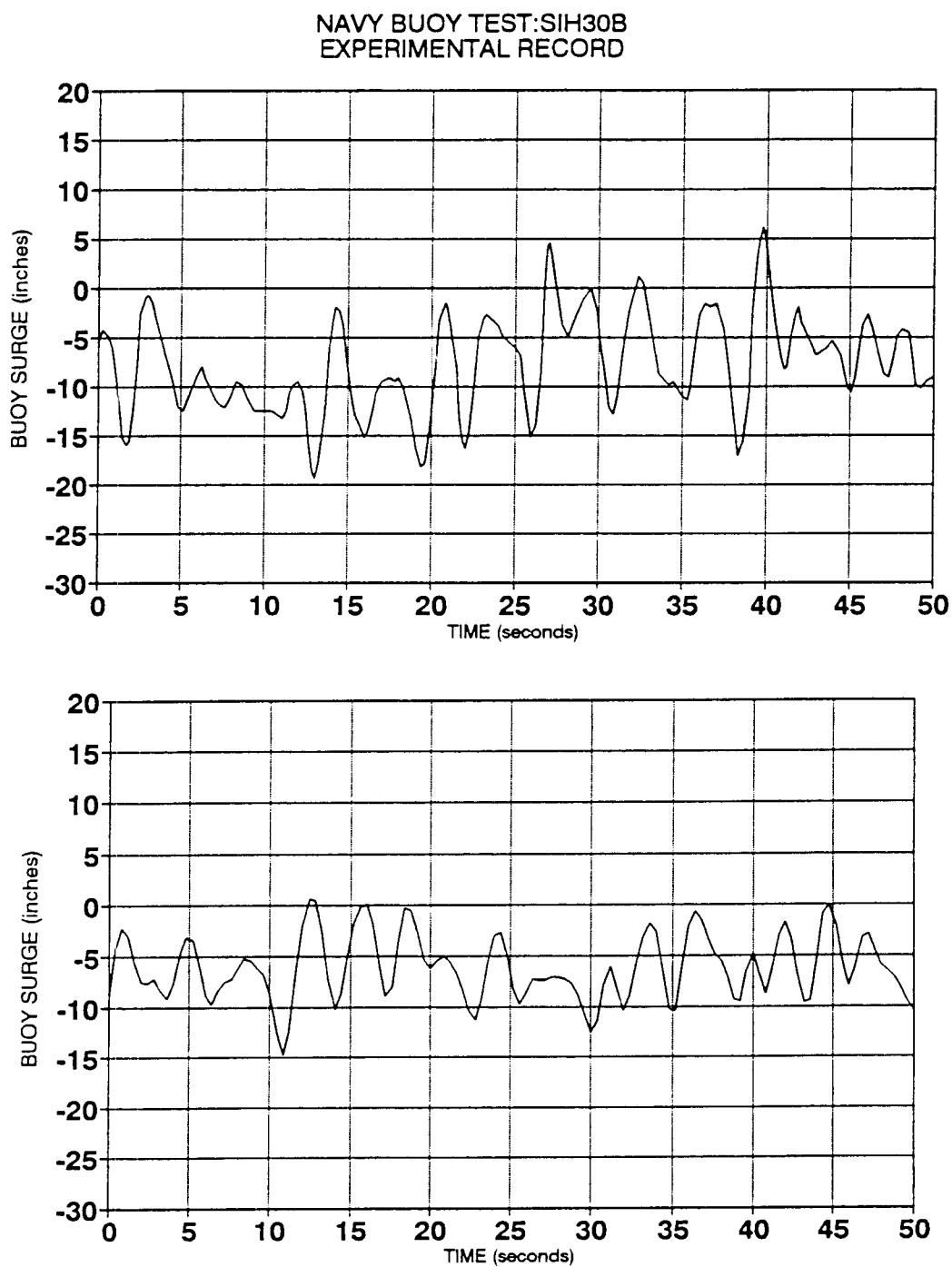
NAVY BUOY TEST:SIH30B
EXPERIMENTAL RECORD

Figure 4.10 Random Response of Surface Buoy Surge

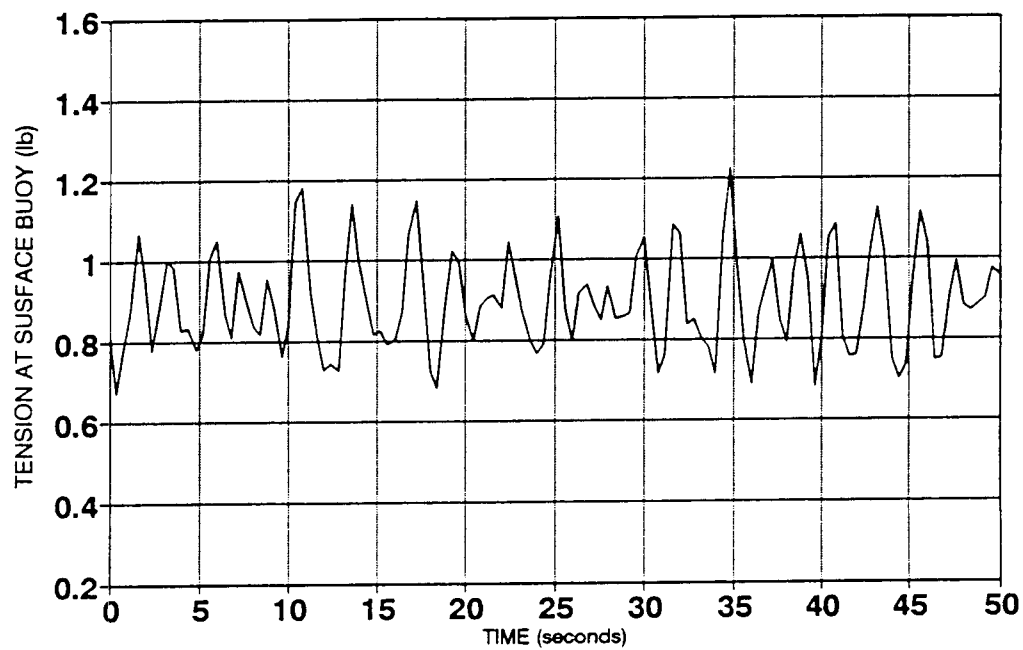(Numerical vs. Experimental Solution)

Figure 4.11 The Random Response of Tension at Top of the Mooring Line

4.3 Problem 3: Towed Cable/Object

The example depicted in Fig.4.12 is used to demonstrate the program capability of dealing with a 2-D towing problem. At time t=0, the tow vessel is in a standstill condition and the cable is in a vertical straight line configuration. The vessel then undergoes constant acceleration of 0.025 m/sec² until it reaches a steady towing speed of 1.5 m/s. The input data for the cable and towed object are summarized as follows:

Mass density of water   = 1020.0 kg/m³

Cable:

Unstretched length	= 20.0 m
Diameter	= 0.04064 m
Mass per unit length	= 1.338021 kg/m
Buoyant weight per unit length	= 0.14594 N/m
Modulus of elasticity	= inextensible
Normal Drag coefficient	= 1.2
Tangential drag coefficient	= 0.015
Added mass coefficient	= 1.0

Object:

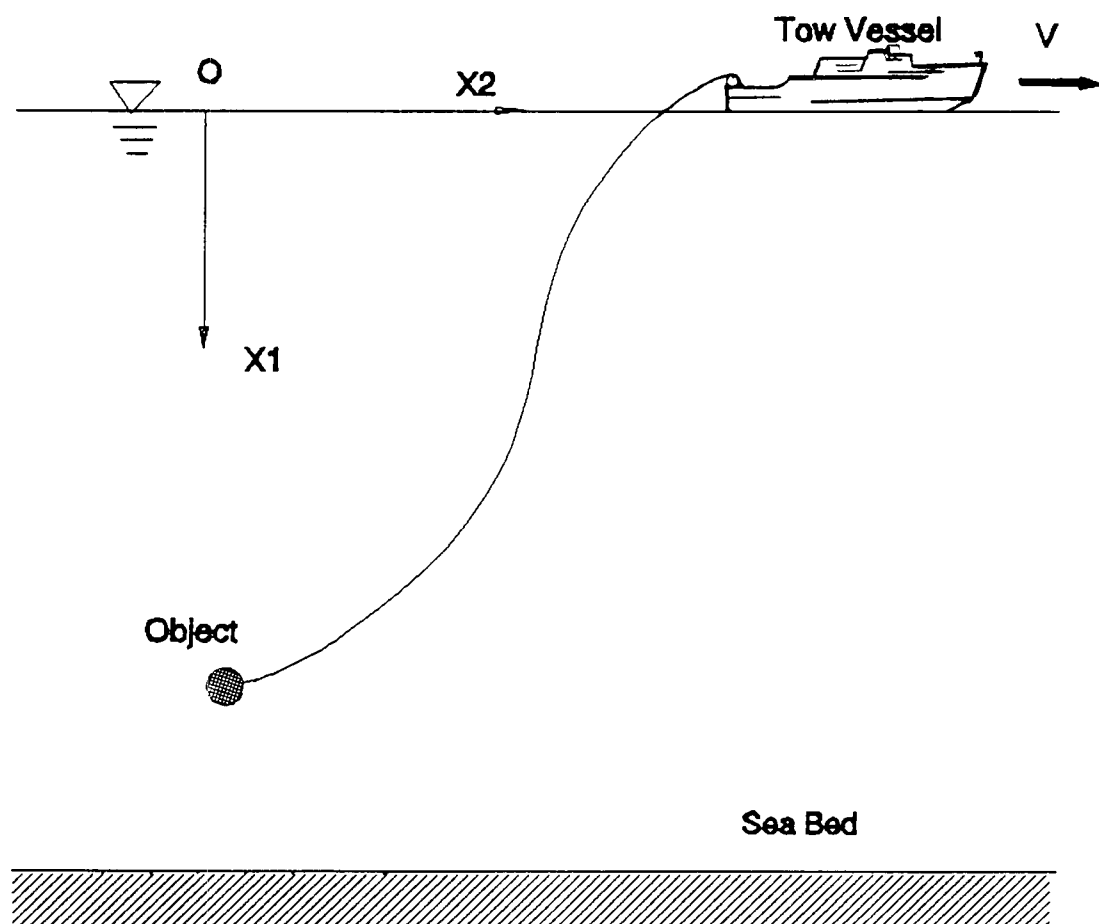|	
Radius	= 0.5 m
Buoyant weight	= 58.17 N
Drag coefficient	= 0.5
Added mass coefficient	= 0.5

Figure 4.12 Definition Sketch of Towed Cable/Object

The tow process was simulated for a total of 100 seconds with a time step size of 1.0 second. A relative tolerance of 0.05 was selected and convergence was achieved typically in 2 to 3 iterations. Fig. 4.13 shows the deployed cable configurations at various times as the tow speed increases. The results of a similar towing problem with three cable segments,each having different material properties summarized in Table 4.2, is given in Fig.4.14 to illustrate the program capability of dealing with material discontinuity.

Table 4.2 Material Properties for Different Cable Segments

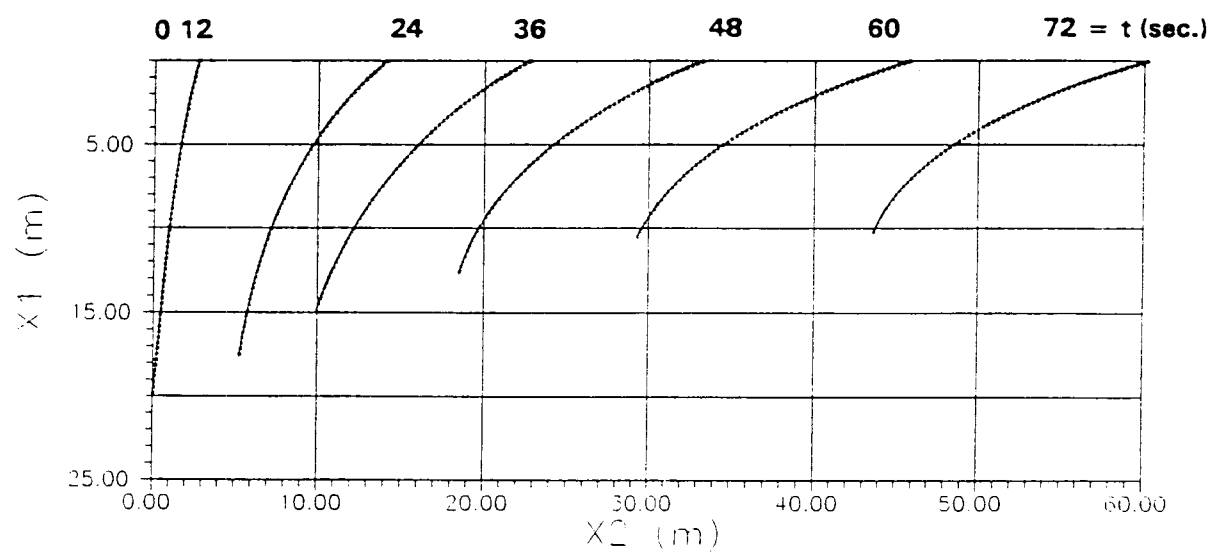| Cable seg. No. Property	I	II	III
cable diameter (m)	0.04064	0.07938	0.0254
segment length (m)	20.0	10.0	10.0
buoyant weight (n/m)	1.14594	0.0	0.03557
mass (kg/m)	1.33802	5.04726	0.52046

Figure 4.13 Deployed Configurations of Towed Cable/Object
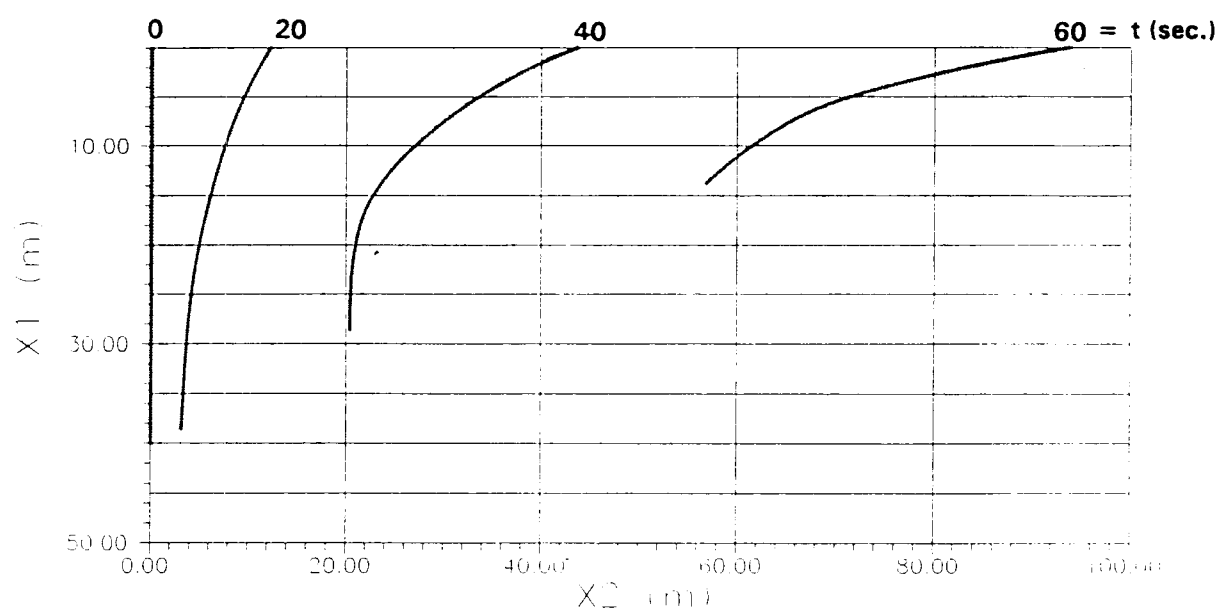
(Time=0 to 72 seconds)

Figure 4.14 Deployed Configurations of Towed Cable/Object

with Three different Cable Segments

4.4 Problem 4: Towed Cable with Free End

This is an illustrative example for testing the free end boundary conditions developed in the Section 2.5.2. As shown in the definition sketch, Fig.4.15, a 40 m long cable with a free end was towed from an initial vertical straight configuration in the absence of surface waves and subsurface currents. The ship velocity was varied linearly from 0.15 m/sec to 1.5 m/sec. The towed cable parameters were selected from the realistic towed array system supplied by Rispin (1980) of the David W. Taylor Naval Ship Research and Development Center (Ablow and Schechter,1983).

The input data are summarized in the following:

Gravitational constant	$= 9.81$ m/s^2
Mass density of water	$= 1020.0$ kg/m^3
Unstretched cable length	$= 40.0$ m
Diameter	$= 0.04064$ m
Mass per unit length	$= 1.561166$ kg/m
Buoyant weight per unit length	$= 2.3350$ N/m
Modulus of elasticity	$=$ inextensible
Normal Drag coefficient	$= 1.2$
Tangential drag coefficient	$= 0.015$
Added mass coefficient	$= 1.0$

To avoid the singularity at the free end, a point P was specified at 1.6 m from the free end. The free end boundary condition were then applied at the point P. From the
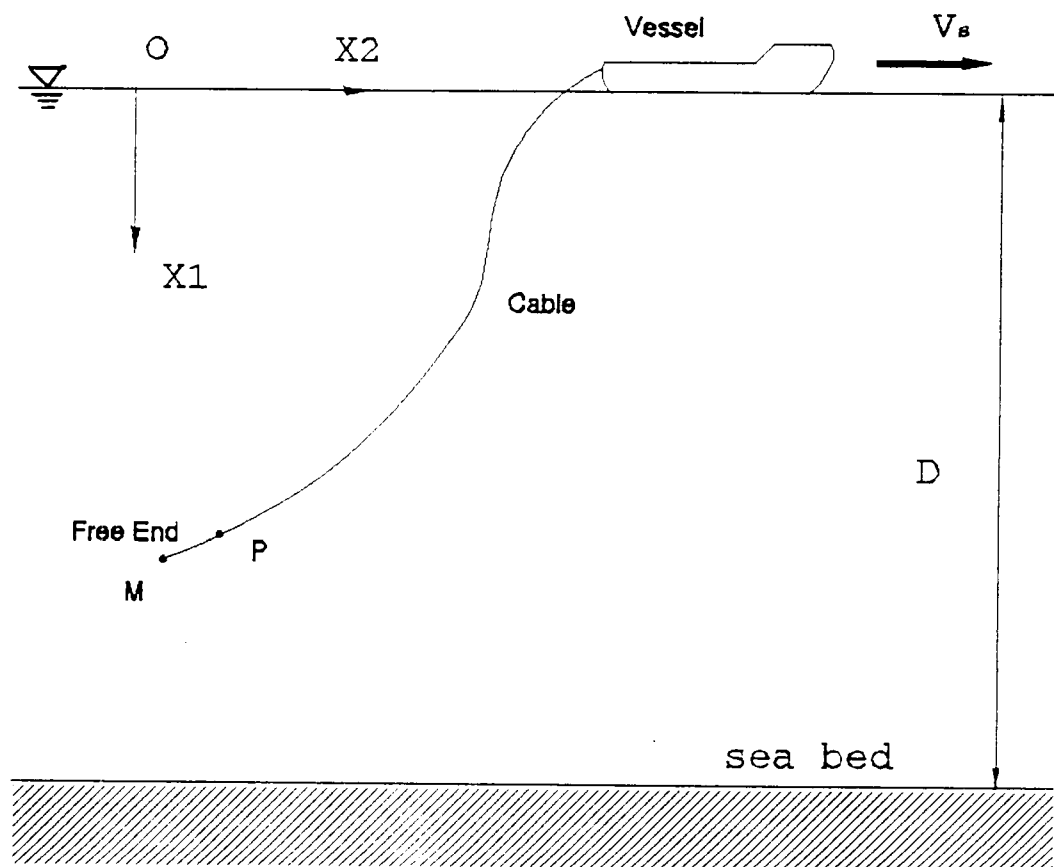
Figure 4.15 Towed Cable with Free End

point P to the free end, the cable is assumed to be a straight line. The velocity components at the free end were calculated by extrapolation. The dynamic simulation was conducted with time step size of 1.0 second. The solution typically converged to 0.05 relative error tolerance in about 3 to 4 iterations. The deployed cable configurations at 10 seconds intervals from 0 to 100 sec. are shown in Fig.4.16.
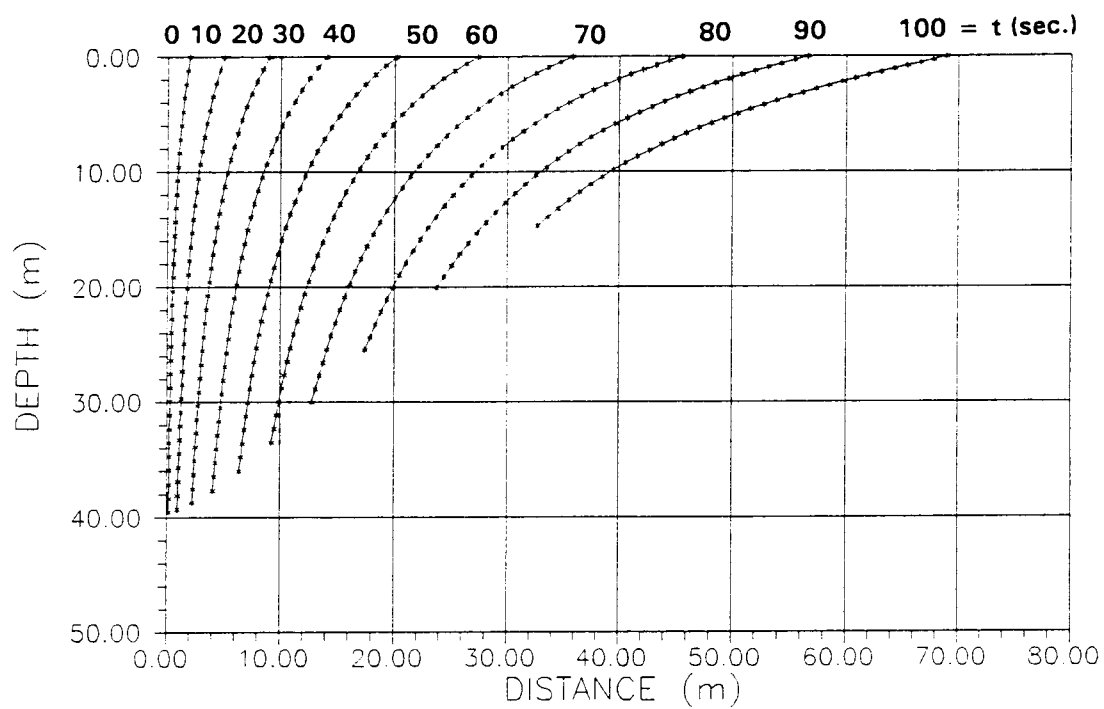
Figure 4.16 Deployed Configurations of Towed Cable with Free End

4.5 Problem 5: Cable/Lumped-Body Payout with Bottom Contact

This example is used to demonstrate the capability of the present solution algorithms to deal with payout boundary conditions and slack-cable/ocean-bottom contact boundary conditions. The example, as depicted in Fig.4.17, is composed of three cable segments and two intermediate bodies. The cable is paid out at a constant payout rate relative to the moving vessel and deposited onto the ocean floor. The same cable parameters as those used in problem 4 were selected. For the first 60 seconds, the system is towed from an initial vertical straight configuration with tow speed varying linearly from 0.15 m/sec to 0.5 m/sec. The payout operation is then started with a constant payout rate of 0.6 m/sec. Because the payout rate is greater than the vessel speed, slack-cable/bottom-contact is expected at the sea floor located at 48 m below the payout point. No surface waves or subsurface currents were considered for this problem.

The input data are summarized in the following:

Gravitational constant	$= 9.81 \text{ m/s}^2$
Mass density of water	$= 1020.0 \text{ kg/m}^3$
Vessel tow speed (ramped)	$= 0.15 \text{ to } 0.5 \text{ m/sec.}$
Start time of payout	$= 60.0 \text{ sec.}$
Payout rate	$= 0.6 \text{ m/sec}$
Water depth	$= 48.0 \text{ m}$
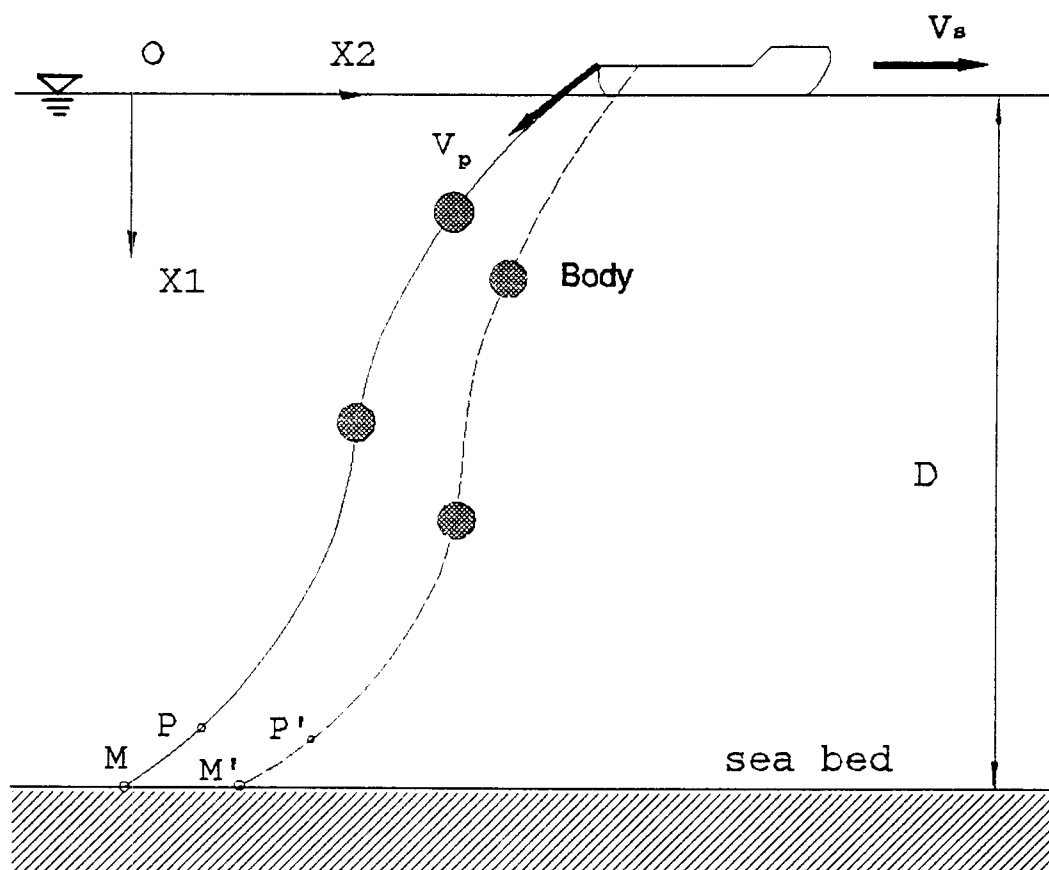
Figure 4.17 Cable/Lumped-Body Payout with Bottom Contact

Cable:

Initial length of each segment	= 7.5, 10.0, 30.0 m
Diameter	= 0.04064 m
Mass per unit length	= 1.561166 kg/m
Buoyant weight per unit length	= 2.3350 N/m
Modulus of elasticity	= inextensible
Normal Drag coefficient	= 1.2
Tangential drag coefficient	= 0.015
Added mass coefficient	= 1.0

Spherical bodies:

Radius	= 0.1 m
Mass	= 6.2726 kg.
Drag coefficient	= 0.5
Added mass coefficient	= 0.5

The numerical integration was performed using a time step size of 2.5 seconds. Convergence was achieved typically in 4 to 8 iterations for the specified 0.01 relative tolerance. Fig.4.18 shows the deployed configuration of cable/lumped-body system at intervals of 5 seconds from 30 to 125 seconds. The system is towed without deployment from 0 to 60 seconds. The bottom contact occurs at time of 70 seconds. The total payout length of the cable is 39 m at a time of 125 seconds (initial length=7.5 m). Curvature changes can be observed when the cable crosses a body. The velocity components profile

and tension magnitude profile at 100 seconds are given in Fig.4.19 and Fig.4.20. The velocity and tension magnitude at the touch-down point are zero because of the assumption that the cable is not dragged along and slack cable is deposited on the ocean bottom. Sudden drops in tension magnitude are shown across the bodies as would be expected.
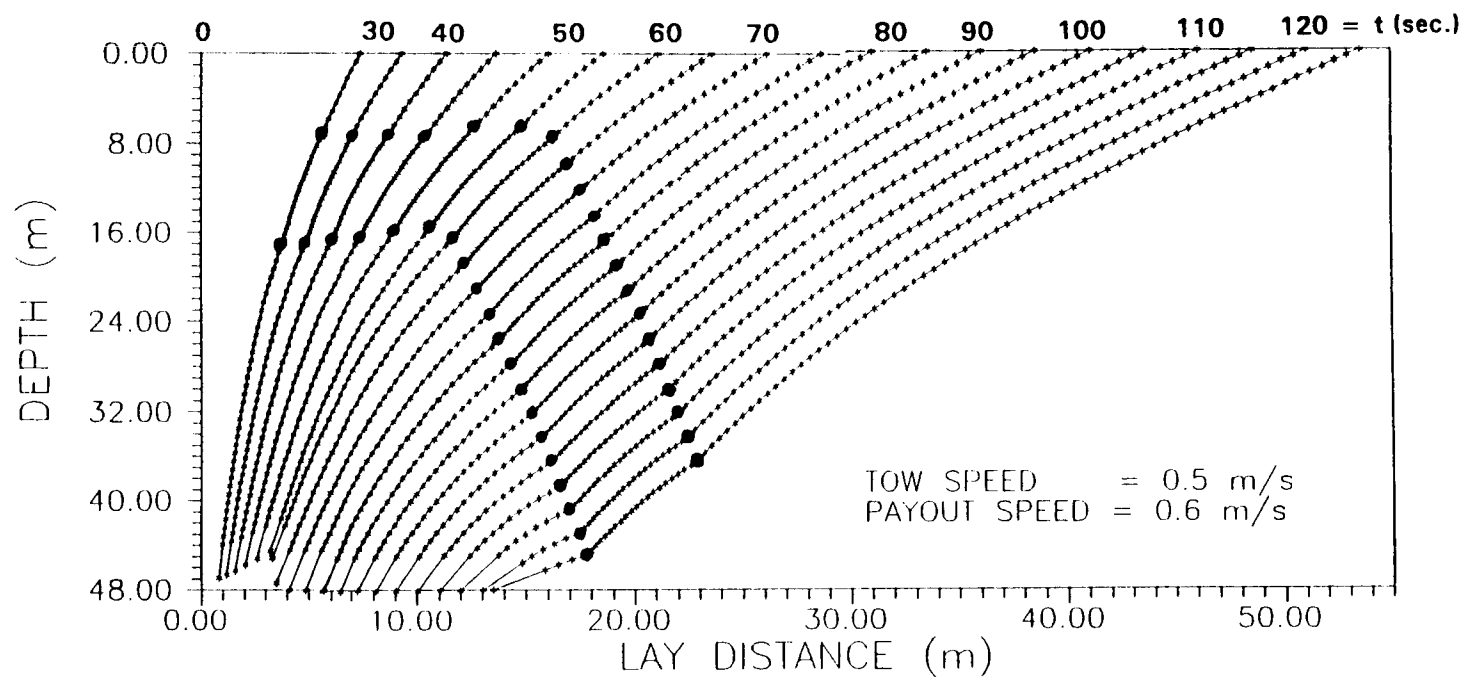
Figure 4.18 Deployed Configurations of Cable/Lumped-Body
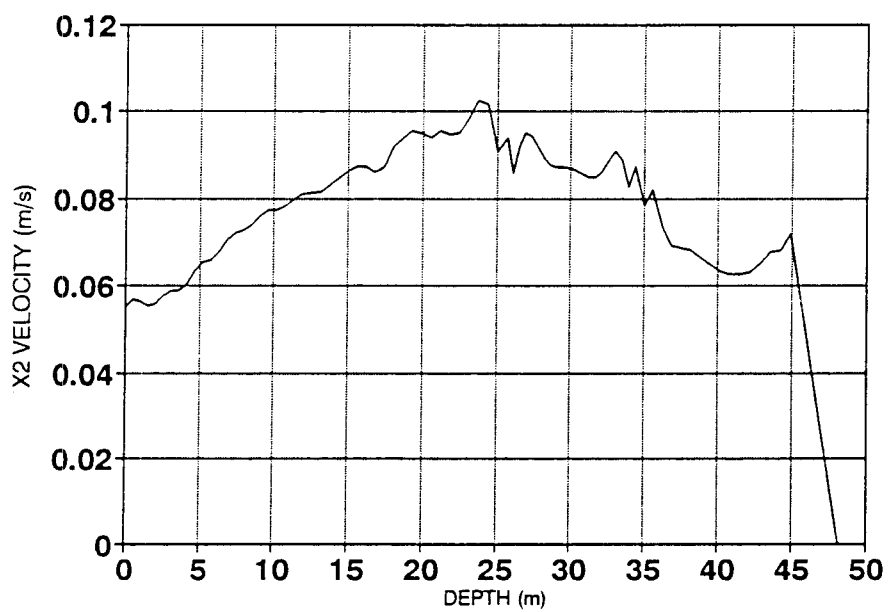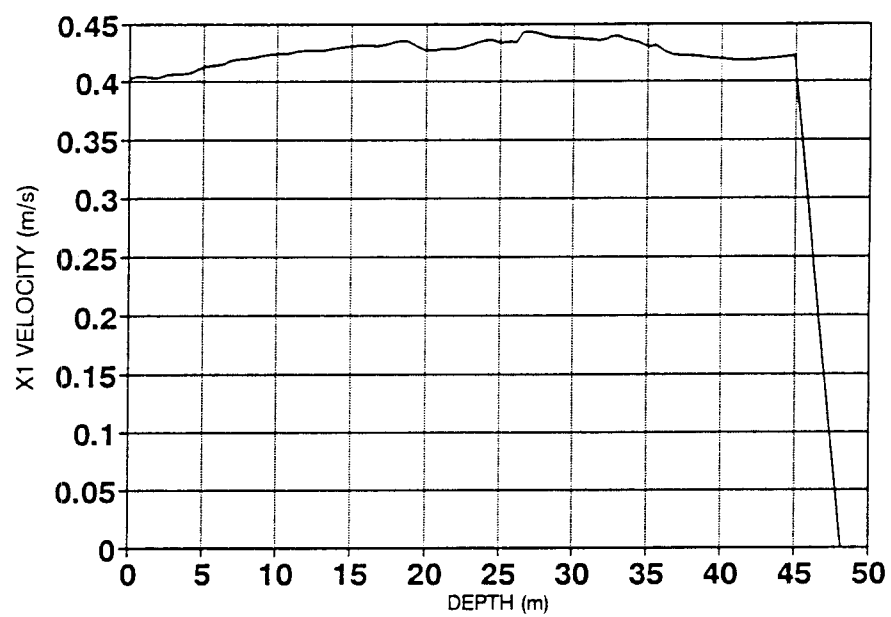
Payout with Bottom Contact (Time= 30 to 125 sec.)
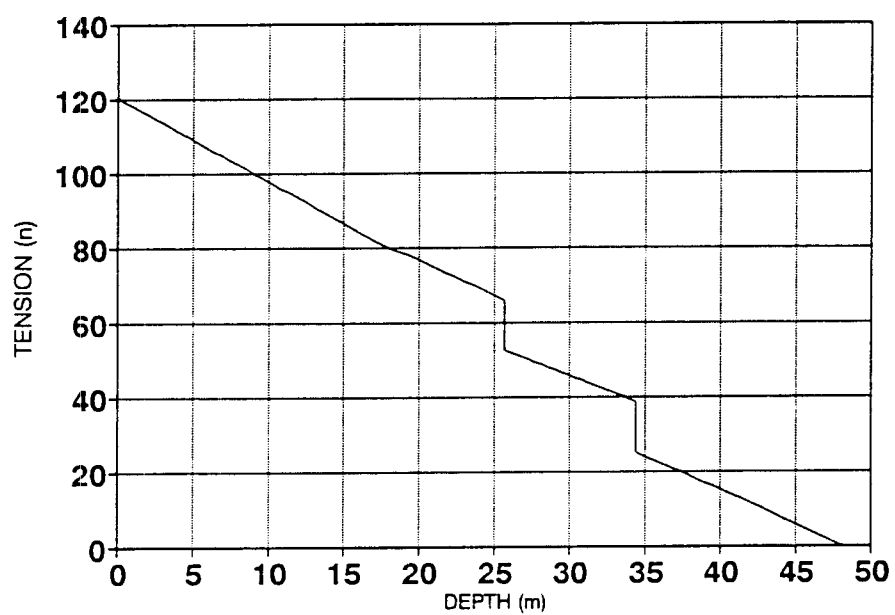
Figure 4.19 Velocity Profiles (Time=100 sec.)

Figure 4.20 Tension Profiles (Time=100 sec.)

5.0 CONCLUSIONS AND RECOMMENDATIONS

5.1 Summary

An improved numerical algorithm for the time-domain simulation of the nonlinear response of a cable/lumped-body system subject to hydrodynamic loadings is developed based on the direct integration method with suppression of extraneous erroneous solution. The main contributions of present study can be summarized as follows:

1) The governing equations of the system are set up from the dynamic equilibrium conditions and kinematic conditions with dependent variables of cable velocity components, direction cosines and tension magnitude such that the potential singularities, i.e. $T=0$, are only present in the equations for the direction cosines. The equations written in such a form provide benefit when dealing with some particular boundary conditions where singularities exist.

2) The numerical damping that exists in KBLDYN is eliminated by introducing a stable Newmark-like implicit integration scheme. The previous integration scheme based on a backward finite difference formula is a special case ($\alpha=0.0$) of the present scheme.

3) The suppression method is used in conjunction with the Newton-Raphson quasi-linearization and decomposition technique for the solution of the quasi-static nonlinear two-point boundary-value problem. The suppression method is shown to be a conceptually simple but efficient numerical technique in controlling the growth of

extraneous erroneous solutions during the direct integration of the partial solutions.

4) The treatment of some special boundary conditions that may be encountered during cable/body installation procedures were investigated. a) The simplified free end boundary conditions are obtained by integrating the cable dynamic equilibrium equation for tension magnitude from the free end to a point P, a short distance from the free end, in order to avoid the singularity at the free end. b) The payout boundary conditions and slack-cable/ocean-bottom contact boundary conditions are included in the present solution algorithm.

5) The "time decremental method" is examined by a numerical example.

6) The validity and capability of the present theoretical formulation and solution algorithm have been shown by examining a set of sample problems and comparing the numerical solutions with available analytical or experimental results.

5.2 Discussion

1) The present formulation based on the dependent variables of velocity components, direction cosines and tension magnitude provide potential benefit in dealing with some particular boundary conditions that may be encountered in the cable deployment problem. However, the direction cosine to be eliminated ϕ_c must be different from zero because it appears in the denominator of Eq.(3.4.2r). It should be chosen such that it does not have zero value within the cable scope at a time step. Therefore, the present solution algorithm fails if the zero values exist within the cable scope for all the direction cosines. For two-dimensional problems, this happens when

both vertical and horizontal cable points exist simultaneously within the cable scope. Fortunately, this situation seldom happens for realistic cable deployment problems.

2) For a system of order 2N, only N dependent variables can be chosen to be suppressed. The choice of these N quantities is arbitrary. Since the direction cosines and tension magnitude are chosen in the present study, there is no direct control of velocity components. The growth of extraneous erroneous velocity components may still be leading to cause instability of the direct integration of partial solutions.

3) By comparing the numerical prediction with the experimental measurements in Example 2, the current numerical model seems to underestimate the buoy motion in general especially for buoy surge motion. This may be attributable to the buoy-water-air interface and buoy rotational effects.

5.3 Future Research Possibilities

Following is a list of important areas where further research is needed.

1). Further investigation is needed regarding the suppression scheme on the direct control of the growth of extraneous erroneous velocity components.

2) The numerical simulation of actively controlled cable deployment should be further modified to include the simulation of the body being paid out from the moving vessel or deposited onto the inclined ocean floor. In such a case, not only the cable integration scope and the water depth are variable but also the problem definition changes as the payout operation proceeds.

3) In the simulation of the cable installation problems, it is the values at a

future "desired" status that are most important, rather than the history of how they were obtained. Therefore, it is highly desirable to successfully implement the "time decremental method" (Leonard,1989) in the present numerical model for the cable/lumped-body systems. Further investigation is required regarding its numerical stability.

4) It is necessary to combine the present study with that made to enhance the treatment of buoy rotational effects to provide a more accurate computer simulation program of moored buoy response.

REFERENCES

1. Ahmed, H.U., "Numerical Integration of Large Deflection Elastic-Plastic Axisymmetric Shells of Revolution", Ph.D. Dissertation, IIT, 1976.

2. Akkari, M.M., "Nonlinear Dynamic Analysis Using Mode Superposition", Ph.D. Dissertation, University of California at Davis, CA, 1983.

3. Albow, C.M. and Schechter, S., "Numerical Simulation of Undersea Cable Dynamics", Ocean Engineering, Vol, 10, 1983, pp. 443-475.

4. Ansari, K.A., "Mooring with Multicomponent Cable Systems", Journal of Energy Resources Technology, Transactions of ASME, Vol. 102, 1980, pp. 62-69.

5. Ansari, K.A., and Khan, N.U., "The Effect of Cable Dynamics on the Station-Keeping Response of a Moored Offshore Vessel," Journal of Energy Resources Technology, Vol. 108, 1986, pp. 52-58.

6. Bathe, K.J., Finite Element Procedures in Engineering Analysis, Prentice-Hall, 1984.

7. Berteaux, H.O., Buoy Engineering, John Wuley & Sons, 1976.

8. Burgess, J.J., "Natural Modes and Impulsive Motions of a Horizontal Shallow Sag Cable", Ph.D. Dissertation, MIT, 1985.

9. Carter, R.L., Robinson, A.R. and Schnobrich, W.C., "Free and Forced Vibrations of Hyperbolical Shells, of Revolutions", ASCE Journal of Eng. Mech. Div., Vol. 95, No. EM 5, Oct 1969, pp.1033-1054.

10. Chakrabarti, S.K., Hydrodynamics of Offshore Structures, Computational Mechanics Publications, Southampton Boston, 1987.

11. Chiou, R. "Nonlinear Static Analysis of Long Submerged Cable Segments by Spatial Integration", M.S., Oregon State University, 1985.

12. Chiou, R., "Nonlinear Hydrodynamic Response of Curved Singly-Connected Cables", Ph.D. Dissertation, OSU, 1989.

13. Clough, R.W. and Penzien, J., Dynamics of Structures, McGraw-Hill Book Co., New York, 1975.

14. Cook, R.D., Concepts and Applications of Finite Element Analysis, 2nd edition,

John Wiley & Sons, 1981.

15. Dean, R.G. and Dalrymple, R.A, Water Wave Mechanics for Engineers and Scientists, Prentice-Hall, Inc., Englewood Cliffs, New Jersey.

16. Delmer, T.N. and Stephens, T.C., "Numerical Simulation of Towed Cables", Ocean Engineering, Vol. 10, 1983, pp. 119-132.

17. Delmer, T.N. and Stephens, T.C., "Numerical Simulation of an Oscillating Towed Weight", Ocean Engineering, Vol. 16, 1989, pp.143-172.

18. Delmer, T.N., Stephens, T.C., and Tremills, J.A., "Numerical Simulation of Cable-Towed Acoustic Arrays", Ocean Engineering, Vol. 15, 1988, pp. 511-548.

19. Garrison, C.J., Field, J.B., and May, M.D., "Drag and Inertia Forces on a Cylinder in a Periodic Flow, Journal of Waterway, Port, Coastal and Ocean Division, ASCE, Vol. 103, 1977, pp. 193-204.

20. Gerald, C.F. and Wheatley, P.O., Applied Numerical Analysis, 3rd edition, Addison-Wesley, 1984.

21. Gerdeen, J.C., Simonen, F.A. and Hunter, D.T., "Large Deflection Analysis of Elastic-Plastic Shells Using Numerical Integration," AIAA J. Vol. 9, No. 6, June 1970, pp. 1012-1018.

22. Goldberg, J.E., and Bogdanoff, J.L., "Static and Dynamic Analysis of Nonuniform Conical Shells Under Symmetrical and Unsymmetrical Conditions," Proc., Sixth Symposium on Ballistic Missile and Aerospace Technology, Vol.1, Academic press, New York, 1961, pp. 219-238.

23. Hooft, J.P., "Computer Simulations of the Behavior of Maritime Structures", Marine Technology, Vol. 23, 1986, pp. 139-157.

24. Hudspeth, R.T., "Environmental Forces on Ocean Platforms", Report N-1681, Naval Civil Engineering Laboratory, Port Hueneme, Californiia, 1983, pp. 27-84.

25. Huston, R.L. and Kamman, J.W., "Validation of Finite Segment Cable Models", Computers and Structures, Vol. 15, 1982, pp. 653-660.

26. Kamman, J.W. and Huston, R.L., "Modelling of Submerged Cable Dynamics", Computers and Structures, Vol. 20, 1985, pp. 623-629.

27. Kern, E.C., Jr, Milgram, J.H., and Lincoln, W.B., "Experimental Determination of the Dynamics of a Mooring System", Journal of Hydronautics, Vol. 11, 1977,

pp. 113-120.

28. Knapp, R.H., "Cable System", <u>Mechanical Engineering</u>, ASME, February, 1987, pp. 76-79.

29. Lee, E.S., "Quasi-Linearization, Non-Linear Boundary Value Problems and Optimization", <u>Chemical Engineering Science</u>, Vol. 21, 1966, pp. 183-194.

30. Leonard, J.W., "Dynamic Response of Initially-Stressed Membrane Shells", <u>ASCE Journal of Struc. Div.</u>, Vol. 99, No. ST 12, Dec 1968, pp. 2861-2883.

31. Leonard, J.W., "Newton-Raphson Iterative Method Applied to Circularly Towed Cable-Body System", <u>Engineering Structures</u>, 1979, pp. 73-80.

32. Leonard. J.W., "Review of Preliminary Analysis Techniques for Tension Structures", <u>NCEL Report CT 84.071</u>, Oregon State Univ., Dept. of Civil Engineering, Corvallis, Oregon, 1984.

33. Leonard, J.W., <u>Tension Structures:Behavior and Analysis</u>, McGraw-Hill, New York, New York, 1988.

34. Leonard. J.W., "Feasibility of Time Decrement Methods for Expeditions Cable Installation Technology", <u>Report Submitted to NCEL</u>, September 1989.

35. Leonard, J.W., Garrison, C.J. and Hudspeth, R.T., "Deterministic Fluid Forces on Structures: A Review", <u>Journal of the Structural Division</u>, ASCE, Vol. 107, 1981, pp. 1041-1057.

36. Leonard, J.W. and Hudspeth, R.T., "Dynamic Response of Small Buoys to Ocean Surface Waves", <u>Research Proposal Submitted to Naval Civil Engineering Laboratory</u>, 1989.

37. Leonard, J.W. and Nath, J.H., "Comparison of Finite Element and Lumped Parameter Methods for Oceanic Cables", <u>Engineering Structures</u>, Vol. 3, 1981, pp. 153-167.

38. Leonard, J.W. amd Recker. W.W., "Nonlinear Dynamics of Cables with Low Initial Tension", <u>Journal of Engineering Mechanics Division</u>, ASCE, Vol. 98, 1972, pp. 293-309.

39. Leonard J.W. and Yim, S.C.S., "Advanced Ocean Ranges Technology, Expeditions Installation Technology for Cable/Lumped-Body Systems", <u>Research Proposal Submitted to Naval Civil Engineering Laboratory</u>, 1989.

40. Liu, F.C.,"Establishment of Initial Configurations in Lumped Parameter Simulations of Underwater Cable Dynamics", <u>Technical Memo M-44-77-9</u>, Naval Civil Engineering Laboratory, Port Hueneme, California, 1977.

41. Liu, F.C., "SNAPLD User's Manual, A Computer Program for the Simulation of Oceanic Cable Systems", <u>Technical Note TN NO. N-1619</u>, Naval Civil Engineering Laboratory, Port Hueneme, California, 1982.

42. Lo, A., "Nonlinear Dynamic Analysis Of Cable and Membrane Structures", a thesis submitted to Oregon State University in partial fulfillment of the requirements for the degree of Doctor of Philosophy, June 1982.

43. Meggitt, D.J., Palo, P.A., and Buck, E.F., "Small-Size Laboratory Experiments on the Large-Displacement Dynamics of Cable Systems", <u>CEL Technical Memorandum M-44-78-11</u>, Vol. I, 1978.

44. Meggitt, D.J., Palo, P.A., Buck, E.F., and Lacroce, P., Small-Size Laboratory Experiments on the Large-Displacement Dynamics of Cable Systems", <u>CEL Technical Memorandum M-44-79 1</u>, Vol. II-A,1978.

45. Migliore, H.J. and Webster, R.L.,"Current Methods for Analyzing Dynamics Cable Response ", <u>Shock and Vibration Digest</u>, Vol. 11, 1979, pp. 3-16.

46. Morison, J.R., O'Brien, M.P., Johnson, J.W. and Schaaf, S.A., 'The Force Exerted by Surface Waves on Piles", <u>Petroleum Transactions</u>, AIME, Vol. 189, 1950, pp. 149-154.

47. Nath, J.H., "Tether Element Geometry from Steady Loads", <u>Journal of the Waterway Port Coastal and Ocean Division</u>, ASCE, Vol. 105, WW2, 1979, pp. 193-197.

48. Nath, J.H. and Thresher, R.W., "Anchor-Last Deployment for Buoy Moorings", <u>Paper No. OTC 2364</u>, Offshore Technology Conference, Dallas, Texas, 1975, pp. 273-283.

49. Palo, P.A., "Small-Scale Cable Dynamics Comparisons", Proceedings, <u>Civil Engineering in the Oceans IV</u>, Vol. I, September, 1979, pp. 293-308.

50. Palo, P.A., "Development of a General-Purpose Mooring Analysis Capability for the U.S. Navy", Presented at San Diego Section of Society of Naval Architects and Marine Engineers meeting, February 1985.

51. Peregrine, D.H., "Interaction of Water Waves and Currents", <u>Advanced in Applied Mechanics</u>, Vol. 16, 1976, pp. 9-117.

52. PMB, Description of SEASTAR Program, private communications with J.W. Leonard and D.R. Shields, 1989.

53. Press, W.H., Flannery, B.P., Teukolsky, S.A., and Vetterling, W.T., Numerical Recipes, Cambridge University Press, New York, New York, 1986.

54. Rajabi, F. and Mangiavacchi, A., "Model Test of a Pile-Founded Guyed Tower", Paper No.OTC 5675, Offshore Technology Conference, Houston, Texas, 1988, pp. 531-542.

55. Rayleigh, J.W.C., Theory of Sound, Second edition, Vol. I, Dover Publications, New York, New York, 1945.

56. Sanders, J.W., "A Three-Dimensional Dynamic Analysis of a Towed System", Ocean Engineering, Vol. 0, 1982, pp. 483-499.

57. Sarpkaya, T., "In-Line and Transverse Forces on Cylinders in Oscillating Flow at High Reynolds Numbers", OTC 2533, Proceedings of the Eighth Offshore Technology Conference, Houston, Texas, 1976, pp. 95-108.

58. Sarpkaya, T., Bakmis, C., and Storm, M.A., "Hydrodynamic Forces from Combined Wave and Current Flow on Smooth and Rough Circular Cylinders at High Reynolds Number", OTC 4830, Proceedings of the Sixteenth Offshore Technology Conference, Houston, Texas, 1984, pp. 455-462.

59. Sarpkaya, T. and Isaacson, M., Mechanics of Wave Forces on Offshore Structures, Van Nostrand Reinhold Company, New York, New York, 1981.

60. Shields, D.R., "NCEL Ocean Platform Seminar", Report N-1681, Naval Civil Engineering Laboratory, Port Hueneme, California, 1983.

61. Shugar, T.A., and Armand, J.L., "Computational Methods in Ocean Structural Engineering - A Review", Report TN 1768, Naval Civil Engineering Laboratory, Port Hueneme, California, 1987.

62. Simpson, R. and Leonard, J.W., "Combined and Torsion in Long Oceanic Cables", Proceedings of Ocean Tension Structural Dynamics Symposium, Oregon State University, Corvallis, Oregon, 1988, pp. 206-230.

63. Skop, R.A. and O'Hara, G.J., "The Method of Imaginary Reactions: A New Technique for Analyzing Structural Cable System", Marine Technology Society Journal, Vol. 4, 1970, pp. 21-30.

64. Thresher, R.W. and Nath, J.H., "Anchor-Last Deployment Simulation by

Lumped Masses", *Journal of the Waterways, Harbors and Coastal Engineering Division*, ASCE, Vol, 1975, pp. 419-433.

65. Tuah, H., "Cable Dynamics in an Ocean Environment", a thesis submitted to Oregon State University in partial fulfillment of the requirements for the degree of Doctor of Philosophy, June 1983.

66. Wadsworth, J.F., III, "A Compendium of Tension Member Properties for Input to Cable Structures Analysis Program", *Report CR 82.017*, Naval Civil Engineering Laboratory, Port Hueneme, California, 1982.

67. Wang, H.T., "A FORTRAN IV Computer Program for the Time Domain Analysis of the Two-Dimensional Dynamic Motions of General Buoy-Cable-Buoy Systems", *Report 77-0046*, David W.Taylor Naval Ship Research and Development Center, Bethesda, MD, 1977.

68. Wang. H.T., "Three-Dimensional Long-Time Motion Behavior of Ocean Cable Systems", *Proceedings of the Second International Offshore* Mechanics and Arctic Engineering Symposium, 1983, pp. 266-274.

69. Webster, R.L., "Nonlinear Static and Dynamic Response of Underwater Cable Structures Using the Finite Element Method", *OTC 2322*, Offshore Technology Conference, Dallas, Texas, 1975, pp. 753-764.

70. Webster, R.L. and Palo, P.A., "SEADYN User's Manual", *NCEL Technical Note N-1630*, Port Hueneme, California, 1982.

71. Webster. R.L. and Palo, P.A., "Experiences in the Development of a General-Purpose Mooring Analysis Capability", *Proceedings of Ocean Structural Dynamics Symposium*, Oregon State University, Corvallis, Oregon, 1986, pp. 421-435.

72. Wilson, B.W. and Garbaccio, D. H., "Dynamics of Ship Anchor-Lines in Waves and Current", *Journal of the Waterways and Harbors Division*, ASCE, Vol. 95, WW4, 1969,pp. 449-465.

73. Yashima, N., Matsunaga, E., and Nakamura, M., "A Large-Scale Model Test of Turret Mooring System for Floating Production Storage Offloading (FPSOO", *OTC 5980*, Offshore Technology Conference, Houston, Texas, 1989, pp. 223-232.

74. Yoon, T.Y. and Leonard J.W., "Natural Vibrations of Cables in a Flowing Fluid", *Report No. OE-87-52*, Oregon State University, Corvallis, Oregon, 1987.

75. Zarghamee, M.S. and Robinson, A.R., "Free and Forced Vibrations of Spherical Shells", <u>Journal of American Institute of Aeronautics</u>, Vol. 5, No.7, July 1967, pp. 1256-1261.